

Fatigue Characterization of Asphalt Mixes with Polymer Modified Asphalt Cement

by

Ali Qabur

A thesis
presented to the University of Waterloo
in fulfillment of the
thesis requirement for the degree of
Master of Applied Science
in
Civil Engineering

Waterloo, Ontario, Canada, 2018

©Ali Qabur 2018

Author's Declaration

I hereby declare that I am the sole author of this thesis. This is a true copy of the thesis, including any required final revisions, as accepted by my examiners.

I understand that my thesis may be made electronically available to the public.

Abstract

Asphalt pavement cracking is the most prevalent distress in pavements. In flexible pavements, fatigue cracking is a major cause of deterioration and can significantly reduce the service life of pavements [1]. Fatigue cracking is caused by traffic loading and can be accelerated by aging of the asphalt, freeze-thaw cycles, and poorly designed asphalt concrete mixture. Fatigue resistance of asphalt mixes could be improved by adding Polymer Modified Asphalt Cement (PMAC) [2]. In particular, the use of Styrene-Butadiene-Styrene (SBS) was found to be an efficient way to increase the fatigue life of mixes [3]. However, the primary issue is the lack of consistent performance testing methods to determine fatigue performance. In addition, the relationship between the PMAC properties and mixture performance is not fully understood.

This thesis will focus on the evaluation of asphalt mixes with PMAC using the 4 point-bending beam (4PB) test to determine the fatigue performance of asphalt mixtures. The classical fatigue “WÖHLER” curve and “DGCB” damage rate method, which was developed at Département Génie Civil et Bâtiment in Lyon, have been used to evaluate and characterize the fatigue of the asphalt mixes in this study.

In general, it was found that the fatigue life ($N_{f50\%}$) was improved when Polymer Modified Asphalt Cement was used, and the polymer content increased. Both fatigue analysis methods, by WÖHLER curve and the DGCB method, showed that the addition of SBS polymer improved the fatigue life and reduced the damage from fatigue loading. Finally, some recommendations were made with regards to fatigue testing.

Acknowledgements

This thesis would not be achievable without the excellent guidance, caring, and useful comments from Prof. Hassan Baaj who also gave me the opportunity to pursue graduate studies at the Centre for Pavement and Transportation Technology (CPATT). My deepest thanks to you for being such a great and helpful supervisor. I also would like to extend my appreciation to Professors Susan L. Tighe and Adil Al-Mayah for serving as members of the review committee for my thesis.

I sincerely thank the Ministry of Education in Saudi Arabia for their financial help and support throughout my Master's studies.

I would like also to acknowledge the contributions of Yellowline Asphalt Products Ltd. providing the very important in-kind contribution and support in this project, especially by Mike Aurilio.

Also, I would like to express my deepest gratitude to Peter Mikhailenko for his great collaboration and very friendly assistance in the project. I thank all my colleagues at CPATT group and the co-op students for their kind cooperation.

Finally, I would like to thank my parents and my beloved siblings.

Dedication

This thesis is dedicated to my family – my parents, Hussain and Fatimah, and siblings without their love and support this would never have been possible. I am also dedicating this to my beloved Grandmother.

Table of Contents

Author's Declaration	ii
Abstract	iii
Acknowledgements	iv
Dedication	v
List of Figures	viii
List of Tables	x
List of Abbreviations	xi
Chapter 1 INTRODUCTION.....	1
1.1 Background	1
1.2 Problem Statement	4
1.3 Research Objectives	4
1.4 Thesis Organization	5
Chapter 2 LITERATURE REVIEW	6
2.1 Loads Action on Flexible Pavement	6
2.2 Fatigue Cracking of Hot Mix Asphalt.....	7
2.2.1 Loading Frequency	13
2.2.2 Mode of Loading.....	13
2.2.3 Fatigue Failure Criteria	14
2.2.4 Fatigue Test Methods.....	18
2.3 Polymer Modified Asphalt.....	22
2.3.1 Types of Asphalt Modifications.....	23
2.4 Effect of Polymers on Fatigue	28
Chapter 3 METHODOLOGY	30
3.1 Materials Properties and Sample Preparation	31
3.1.1 Asphalt Cement Properties.....	31
3.1.1 SBS Polymers	33
3.1.2 Blending.....	33
3.2 Bending Beam Testing Matrix.....	34
3.2.1 Asphalt Mixtures.....	34
3.2.2 Asphalt Mixture Volumetric Properties.....	37
3.3 Testing Regime	40

3.3.1 4PB Test.....	40
3.4 Fatigue Analysis.....	42
3.4.1 Traditional Method	43
3.4.2 Damage Analysis "DGBC"	44
Chapter 4 RESULTS AND DISCUSSION	47
4.1 Tests Parameters	47
4.1.1 Stiffness (K^*).....	47
4.1.2 Stiffness Modules (E^*).....	49
4.1.1 Actual Strain Level	50
4.1.2 Phase Angle (δ).....	52
4.2 Hot Mix Failure Criteria and Fatigue Life Results	53
4.3 WÖHLER (or Fatigue) Curve and Determination of " ϵ_6 "	55
4.4 Damage Rate Analysis "DGCB".....	59
Chapter 5 CONCLUSIONS, RECOMMENDATIONS AND FUTURE RESEARCH	65
5.1 Conclusions and Recommendations	65
5.2 Future Research	66
References.....	67
Appendices.....	76

List of Figures

Figure 1-1 Basic flexible pavement structure layers [5]	1
Figure 1-2 Estimated asphalt production cost categories[6]	2
Figure 1-3 Flexural fatigue test schematic (Pavement Interactive, 2010).....	3
Figure 2-1 Scheme of traffic loads and corresponding pavement response [18], [19]	6
Figure 2-2 Typical viscoelastic behaviour of asphalt cement [21]	7
Figure 2-3 Typical mechanical behaviour domains of asphalt cement [19], [23].....	8
Figure 2-4 Typical mechanical behaviour domains of asphalt cement [19][23].....	9
Figure 2-5 Typical mechanical behaviour domains of asphalt mixtures [19], [23], [24].....	9
Figure 2-6 Types of fatigue cracking in asphalt pavement [20]	10
Figure 2-7 Fatigued cracking in pavement (Waterloo, Canada).....	11
Figure 2-8 Fatigued cracking pavement “alligator cracking” [28]	12
Figure 2-9 Determination of E_{00i} and a_T from the stiffness evolution curve [15].....	17
Figure 2-10 Determination of W_{00i} and a_w from the dissipated energy curve [15].....	18
Figure 2-11 Determination of W_{00i} and a_w from the dissipated energy curve (Strain control) [59][15].....	18
Figure 2-12 Commonly used fatigue test arrangements [20].....	20
Figure 2-13 Schematic of a Styrene-Butadiene-Styrene (SBS) block copolymer [90].....	27
Figure 2-14 Structure of Styrene-Butadiene-Styrene (SBS) and schematic illustration of reversible crosslinks in SBS with the change in temperature [89]	28
Figure 3-1 Sample of SBS A	33
Figure 3-2 Images of aggregate material composition.....	35
Figure 3-3 PRoSBOX® Shear Compactor at the CPATT Lab, University of Waterloo	36
Figure 3-4 The use of diamond saw for asphalt mix cutting and 380L×63W×50H mm beam specimens .	37
Figure 3-5 Bulk relative density (BRD) determination by (AASHTO T 166 2007a).....	38
Figure 3-6 4PB and Sample set up at the University of Waterloo	41
Figure 3-7 WÖHLER (or fatigue) curve and determination of " ϵ_6 " [15].	43
Figure 3-8 Strain amplitudes " ϵ_6 " giving failure at 1 000 000 cycles from the 11 fatigue tests including the 4-point binding beam (4PB) [12]	44
Figure 4-1 K^*/K_0^* versus $N_{f50\%}$ at 700 $\mu\text{m}/\text{m}$ PG 64-28.....	48
Figure 4-2 K^*/K_0^* versus $N_{f50\%}$ at 700 $\mu\text{m}/\text{m}$ PG 58-28.....	48
Figure 4-3 E^*/E_0^* versus $N_{f50\%}$ at 700 $\mu\text{m}/\text{m}$ PG 64-28.....	49
Figure 4-4 E^*/E_0^* versus $N_{f50\%}$ at 700 $\mu\text{m}/\text{m}$ PG 58-28.....	49

Figure 4-5 K^* and E^* for PG 58-28 and PG 64-28 verses present of polymer at 700 $\mu\text{m}/\text{m}$	50
Figure 4-6 Phase Angle δ ($^\circ$) Versus $N_{f50\%}$ at 700 $\mu\text{m}/\text{m}$ PG 58-28	52
Figure 4-7 Phase Angle δ ($^\circ$) Versus $N_{f50\%}$ at 700 $\mu\text{m}/\text{m}$ PG 64-28	52
Figure 4-8 Comparison of Log $N_{f50\%}$ at 700 $\mu\text{m}/\text{m}$ versus percent polymer for PG 58-28 and PG 64-28.	53
Figure 4-9 $N_{f50\%}$ versus strain level for PG 64-28	54
Figure 4-10 $N_{f50\%}$ versus strain level for PG 58-28	55
Figure 4-11 WÖHLER curve and obtaining " ϵ_6 " for PG 64-28.....	56
Figure 4-12 WÖHLER curve and obtaining " ϵ_6 " for PG 58-28.....	57
Figure 4-13 " ϵ_6 " values for PG 58-28 and PG 64-28.....	58
Figure 4-14 Application for different intervals PG 58-28 SBS A 4% at 700 $\mu\text{m}/\text{m}$	59
Figure 4-15 Damage rate PG 58-28 for interval I1 = (30000 to 60000 cycles)	60
Figure 4-16 Damage rate PG 64-28 for interval I1 = (30000 to 60000 cycles)	60
Figure 4-17 Damage rate PG 58-28 for interval I2 = (40000 to 80000 cycles)	61
Figure 4-18 Damage rate PG 64-28 for interval I2 = (40000 to 80000 cycles)	61
Figure 4-19 Damage rate PG 58-28 for interval I3= (50000 to 150000 cycles)	62
Figure 4-20 Damage rate PG 64-28 for interval I3= (50000 to 150000 cycles)	62
Figure 4-21 Damage rate PG 58-28 for interval I4 = (150000 to 300000 cycles)	63
Figure 4-22 Damage rate PG 64-28 for interval I4 = (150000 to 300000 cycles)	63

List of Tables

Table 2-1 Characteristics of various fatigue tests [57].....	16
Table 2-2 Types of asphalt modifications [81]	24
Table 2-3 Benefits of various modifiers [82].....	25
Table 3-1 Properties of asphalt cement used in PMA preparation [101]	32
Table 3-2 Gradation and volumetric properties of aggregates.....	34
Table 3-3 Asphalt mix formula.....	35
Table 3-4 Mixing and compaction temperatures	36
Table 3-5 HMA mix design properties	40
Table 4-1 Test conditions.....	47
Table 4-2 The desired and actual stain levels	51
Table 4-3 R-Values for PG 58-28.....	64
Table 4-4 R-Values for PG 64-28.....	64

List of Abbreviations

AASHTO	American Association of State Highway and Transportation Officials
CPATT	Centre for Pavement and Transportation Technology
HMA	Hot Mix Asphalt
PMAC	Polymer Modified Asphalt Cement
SBS	Styrene-Butadiene-Styrene
DGCB	Département Génie Civil et Bâtiment
4PB	Four-Point Bending Test
Gmm	Theoretical Maximum Specific Gravity of Loose Mixture
Gsb	Bulk Specific Gravity of the Compacted Mix
Hz	Hertz
MPa	Mega Pascal, N/mm ²
MSCR	Multiple Stress Creep Recovery
MTD	Maximum Relative Theoretical Density
NCHRP	National Cooperative Highway Research Program
NSERC	Natural Science and Engineering Research Council of Canada
RTFO	Rolling Thin-Film Oven
SHRP	Strategic Highway Research Program
Superpave™	Superior Performing Asphalt Pavements
OHMPA	Ontario Asphalt Pavement Council
TAC	Transportation Association of Canada
DSR	Dynamic Shear Rheometer

Chapter 1 INTRODUCTION

1.1 Background

Canada's well-developed transportation system consists of road, rail, water, and air networks. The road network is the most important transportation system, as 90% of all goods are transported in this way. In Canada alone, there are more than 1,420,000 km of roads [4], 200,000 of them are in Ontario (OHMPA, 2012). Approximately 95% of paved roads in the world are being built with or surfaced with asphalt. A conventional flexible pavement structure consists of three main layers: surface course, base course, and sub-base course above the sub-grade "natural ground". For hot mix asphalt (HMA) construction, there are two common methods for pavement layers' full depth HMA and HMA over the aggregate base as shown in Figure 1-2 [5]. The surface course is usually an HMA layer. HMA is a mixture of roughly 95% aggregate and 5% asphalt binder (by mass). An HMA layer can be constructed in single or multiple HMA sub-layers [5]. The surface layer is the stiffest, and significantly contributes to pavement strength. The underlying layers are less stiff but are still important to the pavement structural integrity, as well as for drainage and frost protection.

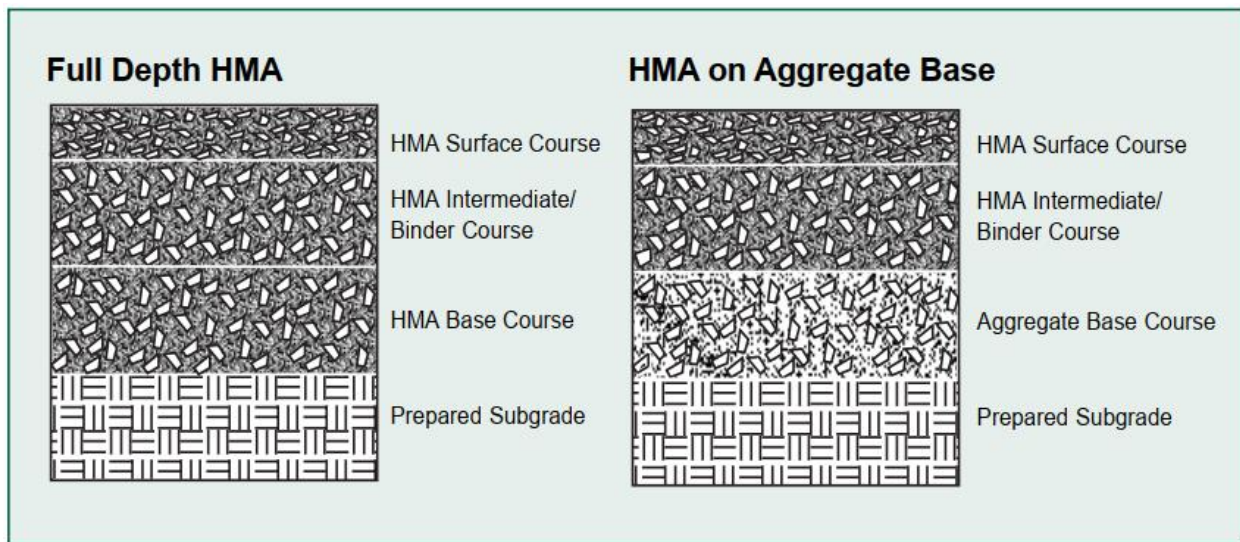


Figure 1-1 Basic flexible pavement structure layers [5]

The cost to produce asphalt concrete is composed of four parts: raw materials, plant production, transportation, and lay-down (i.e. construction). The cost of the materials is commonly the highest

among the four costs, and represents about 70% of the cost to produce HMA as shown in Figure 1-2 [6].

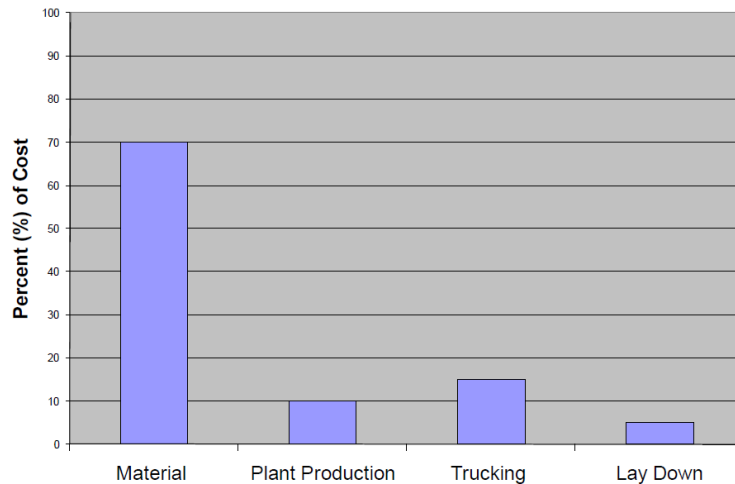


Figure 1-2 Estimated asphalt production cost categories[6]

The most expensive component of HMA is the asphalt binder. The road construction industry is intensely linked to the petroleum industry through the use of asphalt binder, as the price of asphalt binder is interrelated to that of crude oil. High volatility has been seen in the asphalt binder price in recent years according to National Resources Canada (2011). Therefore, it is important to enhance the durability of HMA to reduce the maintenance and rehabilitation costs. To this end, pavement distresses must be controlled effectively. Once this problem is tackled, the need for costly repairs can be mitigated; with the ultimate result being longer-lasting and more durable roads. In addition, the reduction of raw materials, in the long-run, cuts costs and is more environmentally friendly.

Cracking has one of the most deteriorating effects on the roadway network in Canada. General wear and tear accounts for the majority of this type of damage. Fatigue damage is well known as an important factor in the long-term performance of flexible pavements [1], resulting from the accumulation of strain due to repeated loading of vehicles on the pavement. The flexural fatigue test (AASHTO T321) is used to identify the fatigue life of HMA at intermediate pavement operating temperatures (20°C) [7], [8]. As strain accumulates, microcracks begin to form and continue to increase in size, eventually leading to failure in the pavement structure [9]. Thus, fatigue resistance is an important factor for the measurement when developing asphaltic mixtures.

Cracks start at the surface of the pavement when loading is non-uniform or when there is poor bonding between the layers [10]. Additional factors such as poor compaction, low asphalt cement content, mix design issues and aging oxidation also contribute to cracking [11]. During the flexural fatigue test, the beam is subjected to a repeated four-point loading as shown in Figure 1-3.

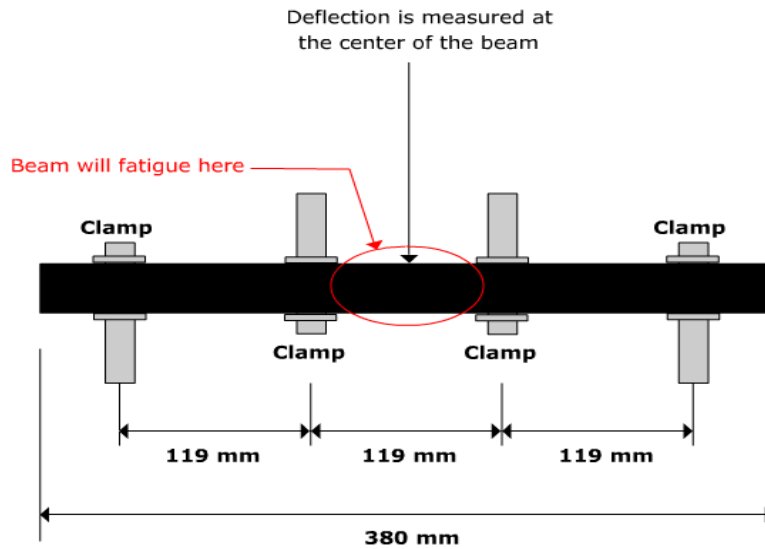


Figure 1-3 Flexural fatigue test schematic (Pavement Interactive, 2010)

It is necessary to investigate the fatigue characterization of HMA containing different concentrations of polymers by utilizing flexural fatigue test. The 4-point bending beam test (4PB) is currently the most commonly used mixture fatigue test in North America. It creates a non-homogeneous stress-strain field which, when combined with other bias effects in fatigue testing itself, could lead to inaccurate findings [12]. The load frequency is usually set between 1 and 10 Hz, and the deflection caused by the loading is measured at the center of the beam. The number of loading cycles applied toward failure can then give an estimate of fatigue life of the HMA beam. As is already known, the measure of failure at 50% in stiffness reduction in 4PB is somewhat arbitrary, because of the way the fatigue performance is extrapolated from the raw data in these tests [13].

Asphalt binders containing higher concentrations of polymers are known to be more strain tolerant and are able to provide improved fatigue resistance in mixtures [14]. Polymer modified asphalt

cement has been used with considerable success to improve fatigue performance [15]. It also improves healing of asphalt mixes during rest periods in fatigue tests, which is an important characteristic with regard to the fatigue life of mixes [3]. However, PMAC developers are challenged to tailor their asphalt formulations for maximum fatigue resistance. Unfortunately, the performance testing methods and the relationship between the binder properties and mixture performance are not fully understood. Studies have shown that polymer modified asphalt cement can improve the fatigue performance of HMA [16].

1.2 Problem Statement

The primary issues are a lack of consistent performance testing methods as well as the approaches that are used to determine the fatigue characteristics of the PMAC. In addition, the relationship between binder properties and mixture performance is not fully understood.

1.3 Research Objectives

The scope of this project has three main components:

- i) To evaluate the fatigue performance of asphalt mixtures with different ratios of PMAC contents,
- ii) To assess the validity of the 4 point-bending beam test in determining fatigue performance of asphalt mixtures,
- iii) To employ the “WÖHLER” Curve and “DGCB” methods in fatigue characterization.

1.4 Thesis Organization

The contents of this thesis are built into five chapters as follows:

- Chapter 1 introduces the study in general, outlines the research, objectives, and scope.
- Chapter 2 provides an extensive review of the literature related to the performance of fatigue and polymer modified asphalt cement. This chapter covers different methods of fatigue analysis, the general concept of polymer modified asphalt, and its effect on fatigue.
- Chapter 3 discusses the research methodology and describes the laboratory testing protocols, the asphalt cements and mixtures, and also describes the performance prediction analysis by introducing failure methods that are used in this research.
- Chapter 4 focuses on laboratory results that are analyzed using the two fatigue analysis methods (“WÖHLER” Curve and “DGCB”).
- Chapter 5 summarizes the research contributions, and provides recommendations for future work.

Chapter 2 LITERATURE REVIEW

2.1 Loads Action on Flexible Pavement

There are two main types of pavements based on their design considerations: flexible pavement and rigid Portland cement concrete pavement. However, this research will only focus on flexible asphalt pavements.

Load distribution can be named as one of the major factors affecting flexible pavement. In order to design a pavement that can maintain structural integrity, the expected loads that a pavement will encounter must be determined properly. Pavement is a layered structure of particular materials that are placed over the foundation soil or subgrade. The main structural purpose of a pavement is to support the wheel loads that lead to creating horizontal tensile stresses and strains at the bottom of a bonded layer, and vertical compressive stresses and strains of HMA. The distribution of the loads to the underlying subgrade is illustrated in Figure 2-1 [17]. The major elements considered in pavement design are: traffic volume, subgrade type and strength, climate, the variety of construction materials available, the anticipated service life, and the thickness of each layer [4].

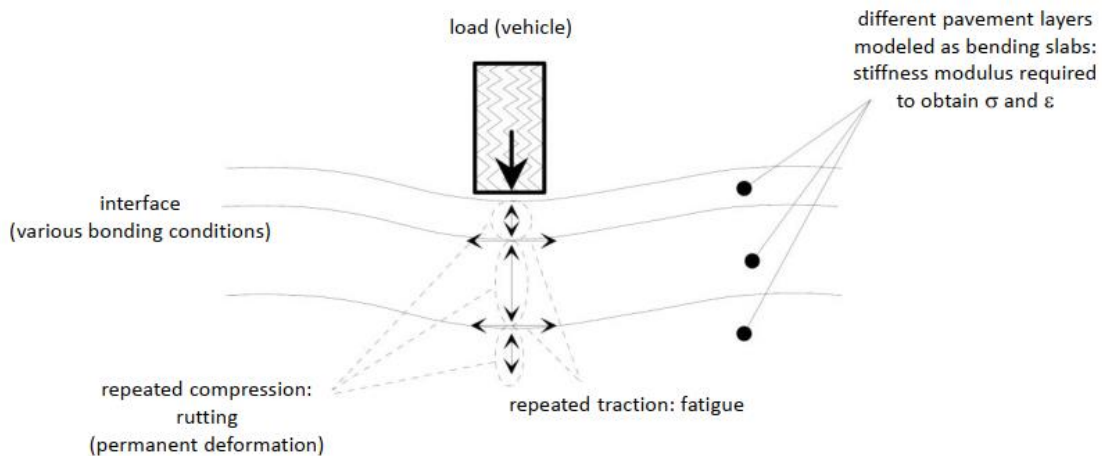


Figure 2-1 Scheme of traffic loads and corresponding pavement response [18], [19]

2.2 Fatigue Cracking of Hot Mix Asphalt

Fatigue cracking is known to be one of the major distresses in asphalt pavements. Fatigue cracking occurs as a result of repetition of traffic-loading on pavement structure. Previous studies have shown that fatigue cracking tends to form at intermediate (i.e. moderate) pavement service temperature. At moderate service temperatures, asphalt cement becomes more stiff and brittle, as opposed to its more viscoelastic behaviour at higher service temperatures, making it more susceptible to cracking from the deformation [20].

As shown in Figure 2-2, asphalt cement is a viscoelastic material that is essentially viscous at higher temperatures, rubber-like and semi-solid at intermediate temperatures, and stiff and brittle at colder temperatures. It is also important to mention that this behaviour is greatly influenced by the type of loading conditions the material is subjected to. For example, asphalt cements exhibit a stiffer response under faster loading rates.

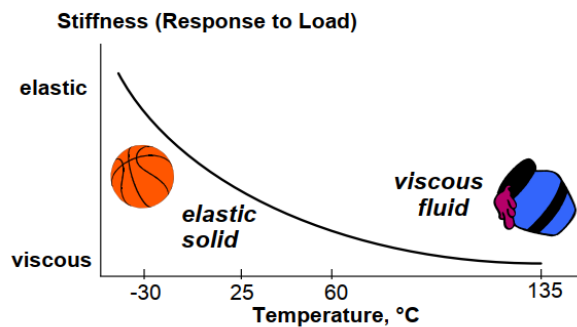


Figure 2-2 Typical viscoelastic behaviour of asphalt cement [21]

Asphalt cement contains some domains of mechanical behaviour; asphalt materials are considered as a continuous, homogeneous, isotropic material. Depending on temperature T , strain amplitude ϵ , and number of loading cycles N , several mechanical behaviour domains can be defined.

Figure 2-3 shows typical mechanical behaviour domains depending on ϵ and T for asphalt binders when the number of cycles N is given [22], [23].

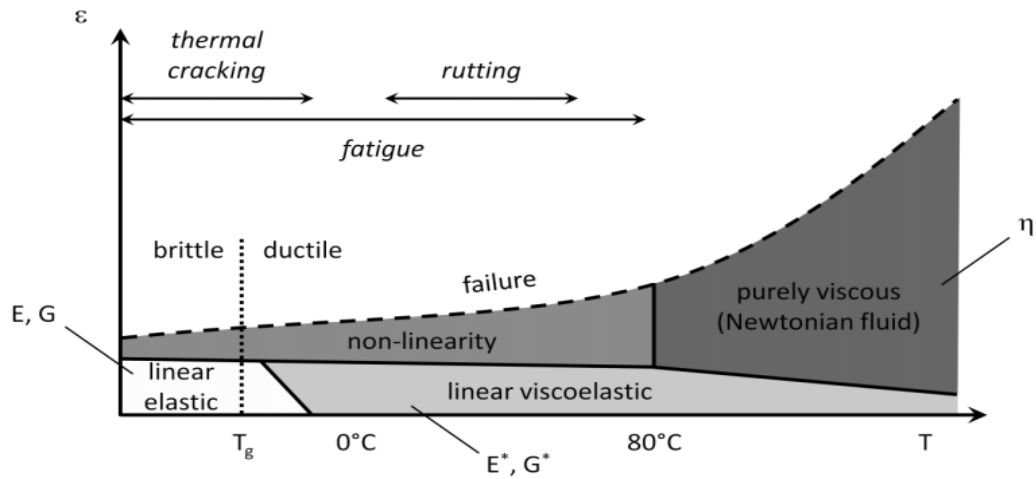


Figure 2-3 Typical mechanical behaviour domains of asphalt cement [19], [23]

The asphalt material and the test temperature play a major role in determining the linear viscoelastic limit of asphalt cement. In contrast, when asphalt cement undergoes a large amplitude strain, the mechanical behaviour becomes non-linear as shown in Figure 2-3. However, the viscous aspect of mechanical behaviour can be ignored at low temperatures, and the substance can be treated as a linear elastic material.

This is not the case when a high number of cycles and large strain amplitudes are present at controlled temperatures, because increased cycles lead to fatigue causing failure as indicated in Figure 2-4.

Having lower strain levels with a lower number of cycles, the asphalt will have a linear viscoelastic behaviour. However, with high strain levels and a lower number of cycles, non-linearity will be observed. Strain levels and number of cycles play an important role in determining fatigue performance. Permanent viscoelastic deformation occurs with high strain levels and an increased number of cycles, whereas fatigue failure is caused by a combination of both.

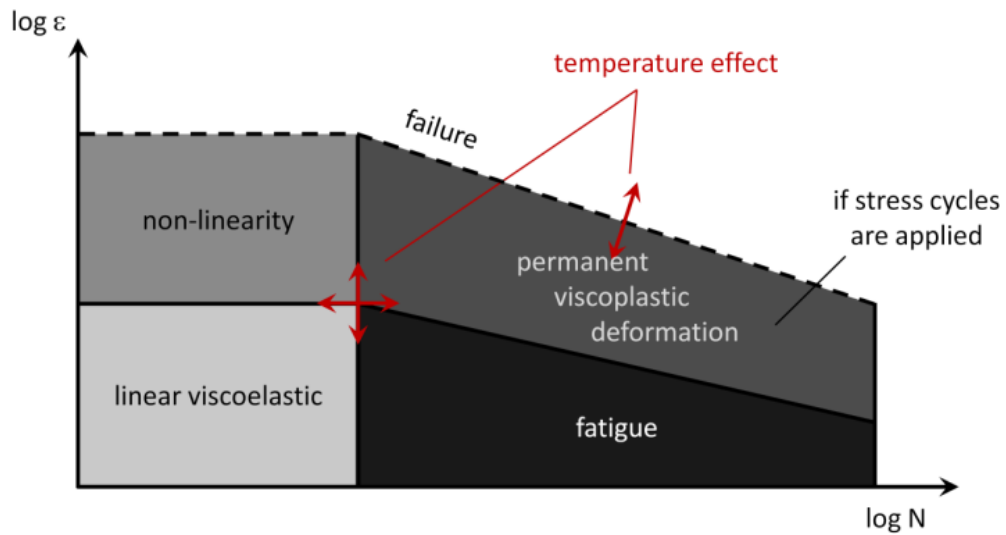


Figure 2-4 Typical mechanical behaviour domains of asphalt cement [19][23]

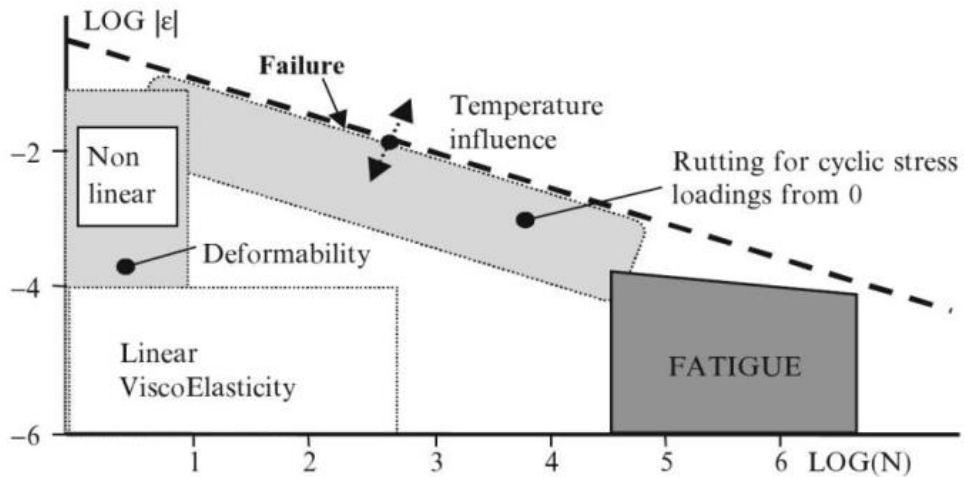


Figure 2-5 Typical mechanical behaviour domains of asphalt mixtures [19], [23], [24]

Figure 2-5 shows the typical mechanical behaviour domains of asphalt mixtures when the temperature T is given and depending on ϵ and N . The properties related to stiffness (complex modulus) can be introduced only when the asphalt mixture behaviour is considered to be linear.

The evaluation of the linear viscoelastic domain of asphalt mixtures is shown in Figure 2-5 when the Y-X axes are a logarithm base 10 of the strain levels and the number of cycles.

This crack development can be classified into two categories: top-down, and bottom-up fatigue cracking as shown in Figure 2-6. Based on the National Cooperative Highway Research Program (NCHRP) publication in 2011, fatigue cracking is defined as cracks that are initiated at the bottom of the pavement layer and gradually grow toward the pavement surface. However, in the past 10 years, pavements are also subject to top-down fatigue cracking, where the cracks begin at or near the pavement surface and grow downward, typically along the edges of the wheel paths. The development of fatigue cracking is entirely a mechanistic process. However, top-down cracking is not as well understood as the more classical “bottom-up” fatigue. From a mechanistic viewpoint, the hypothesis is that certain critical tensile and/or shear stresses develop as a result of extremely large contact pressures at the tire edge-pavement interface. This coupled with a highly aged (stiff), thinly oxidized, thin surface layer is considered to be responsible for the development of top-down surface cracks [25].

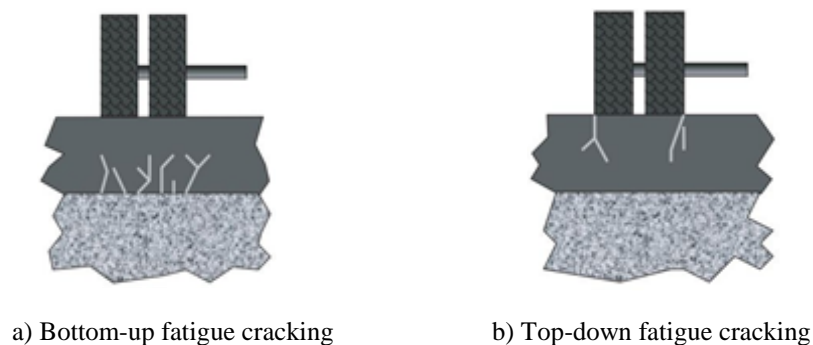


Figure 2-6 Types of fatigue cracking in asphalt pavement [20]

One major contributor to fatigue cracking and premature pavement failure is improper pavement drainage, as stated by [26]. Subsurface pavement layers are often weakened by the intrusion of excessive moisture, thus reducing the stiffness of the entire pavement structure. Of major importance are the large tensile strains induced beneath the HMA layer and the interface layers, due to the action of repeated loading and moisture-damaged subsurface soil layers. These strains

seem to exceed the tensile strength of the asphalt mixture; hence are considered the reason for bottom-up cracking of pavements.

In the design against fatigue cracking, the surface layer binder's structural or physical properties are regarded as a contributing factor to fatigue resistance as described in the manual for design of HMA prepared by NCHRP (2011). This also affects the required HMA pavement thickness. For HMA layers with thicknesses of less than 76 mm (3 in), increasing the high temperature binder stiffness decreases the resistance to both bottom-up and top-down fatigue cracks. On the other hand, increasing the high temperature stiffness increases the resistance to bottom-up fatigue cracking for HMA layers thicker than or equal to 127 mm (5 in).

Failure mechanisms in bottom-up cracking can be described as a three-stage process. It starts with crack initiation, propagation, and final fracture failure. During the crack initiation stage, micro-cracks form and grow until they reach an acute size of ~7.5 mm [27]. This initiation occurs at the region of critical tensile strains and stresses in the pavement. The initial size of a crack may be extremely small and difficult to distinguish from the succeeding stages of propagation, or crack growth. In crack propagation, a single or multiple cracks grow and coalesce to continue the disintegration process. This propagation of fatigue cracking continues and can become interconnected and form alligator cracking as shown in Figure 2-7 and Figure 2-8.



Figure 2-7 Fatigued cracking in pavement (Waterloo, Canada)



Figure 2-8 Fatigued cracking pavement “alligator cracking” [28]

Fatigue cracking in pavements is affected by different external factors such as poor subgrade drainage, method of compaction and placement, and time of placement [29]. In addition, different properties of the mixture including type and amount of binder used in the mixture, temperature, and air voids will influence the fatigue life [30]. As noted by [31], aggregate gradation was a more effective factor for fatigue resistance of asphalt mixture than the effects of asphalt content. A study by [32] shows the effect of aggregate size, 12.5, 19 and 25 mm on three different HMAs. It was observed that the nominal maximum aggregate size of 12.5 mm had the longest fatigue life when used in a mixture. In a related vein, [33] investigated the effects of aggregate size, temperature, and asphalt content on the fatigue characteristic of different asphalt mixtures, hot mix asphalt (HMA) and stone matrix asphalt (SMA). It was observed that HMA mixtures had greater fatigue lives than SMA mixtures because of dense graded aggregate structures which interlocked better to each other in comparison to SMA mixtures.

The fatigue life of pavements is affected by a number of elements such as loading amplitude, compression, frequency and shape of loading, thickness of asphalt layer, and features of asphalt mixtures. These features include stiffness of mixture, additives and environmental conditions, and the sieve analysis for fine and coarse aggregates, as well as the type of binder used [34], [35]. According to [34], as the loading frequency increases, time for self-healing of the materials decreases, which also results in a decrease in the fatigue life of conventional samples, and these relationships are based on the results of strain-controlled tests by four-point bending beam.

2.2.1 Loading Frequency

In order to mimic various speeds of vehicles under a four flexural beam test, the loading frequency has to be modified; typically loading increases when the traffic speed decreases [36]. When the mixtures stiffness is high, the high-frequency is required due to the frequency-dependent stiffness of asphalt mixtures [37]. Thus, more pressure is required in order to achieve a certain level strain in a four-point flexural beam test under a controlled strain mode. In case of high levels of stress, the amount of dissipated energy per load cycle based on energy methods, are more at higher loading frequency when compared to the lower levels of loading frequency [36]. Moreover, higher loading frequencies result in less time for healing asphalt samples [34]. Based on many results from various papers, the fatigue life of conventional asphalt samples was reduced when the loading frequency was increased in four-point flexural beam test under a controlled strain mode [38]

2.2.2 Mode of Loading

The two modes of fatigue loading are the controlled strain (displacement) and controlled stress (force) mode. The loading types are characterized by the ratio R of the minimum force (or displacement) over the maximum force. The ratio R in a sinusoidal and haversine signal loading pattern is characterized as -1 and 0 respectively. Other loading patterns such as square, and triangular-shaped waveforms with or without rest periods have also been used to simulate field traffic load pulses. However, the most commonly used wave forms for characterizing asphalt mixes as well as for the estimation of fatigue life through the development of prediction models are sinusoidal and haversine [17]

For the strain-controlled test, strain amplitude is kept constant at a force that keeps the strain at an initial level. This force gradually decreases after crack initiation, as the flexural stiffness of the mix decreases. The strain-controlled mode of loading simulated conditions in thin asphalt pavement layers, is usually less than 2-inches. In the stress-controlled mode of loading, the stress amplitude is maintained at a constant stress level. This loading initiates an increase in strain amplitude until a point is reached where this amplitude is doubled and flexural stiffness reduced to half its initial value [39].

As demonstrated in [40], fatigue life in the strain control mode is usually greater than for the stress control mode [41]. Absorption of energy in a stress controlled test is high, hence the initial

dissipated energy per cycle is high, and the rate of energy dissipation would be faster. In this manner, variability and scattering of results from the stress controlled test is high. However, if this stress in a controlled stress test is converted to strain, and strain is plotted against the number of cycles to failure, then the scatter is considerably reduced [42]. This suggests that strain controlled tests reduce the scatter and variability associated with fatigue testing. Variability is also associated with sample (test specimen) dimensions, the larger the sample size, the smaller the scatter and variability in the fatigue test results.

2.2.3 Fatigue Failure Criteria

The first laboratory studies about fatigue were performed by [43] on metal chains, but it was Wöhler [44] who first used the word "fatigue" to name the phenomenon. Decades later, [45] investigated the relationship between the magnitude of applied stress repetitions and the number of cycles to failure in metals. It was observed that when a material is subjected to cyclic loading, the number of cycles to failure (also called "fatigue life") decreases when stress amplitude increases. The same observation is valid for several other materials, among which bituminous materials are included. The Wöhler curve is still used and accepted as a standard if fatigue tests are performed in strain control mode.

A large diversity of opinions exists regarding the identification of fatigue failure point (N_f) due to fatigue damage, as can be found in the literature. Depending on the specific fatigue test mode of loading (stress or strain), N_f has been determined in different ways. In the constant stress mode of testing, one definition of N_f was complete fracture at the end of the fatigue test when the specimen fails due to tensile strains [46], [47]. As defined by [48] N_f is the reduction of the initial complex modulus by 90%. Whereas, Van Dijk defines N_f as the number of loading cycles at which the corresponding strain is twice the initial strain [39].

For constant strain mode of testing, several N_f definitions have been adopted. The most common and widely used definition of N_f is the 50% reduction in the initial stiffness [41], [47], [49]. Subsequently, the 50% reduction in stiffness was adopted to define N_f by AASHTO in provisional standard TP8-94 (2002) and AASHTO T 321.

According to Kim et al., the 50% reduction in pseudo stiffness as a failure point in fatigue testing, was believed to be independent of the mode of loading and stress/strain amplitude [50]. Whereas, Reese used phase angle to define the Nf as the cycle at which the phase angle shows a maximum value with time followed by a sharp decrease of Nf [51]. Using this phase angle failure criterion, Daniel [52] found that the midpoint of the failure range occurred at a pseudo stiffness reduction of 29% for a cyclic uniaxial fatigue test and 31% for a monotonic uniaxial test.

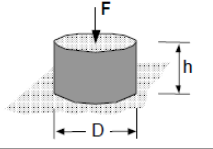
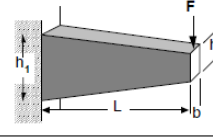
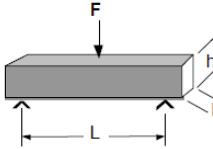
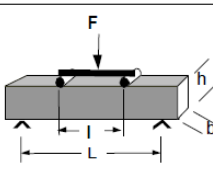
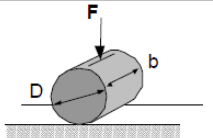
Further studies carried out by [13] identified Nf by plotting the load cycle value n_i versus the load cycle multiplied by the stiffness S_i at that cycle ($n_i \times S_i$). The peak value of the curve is indicated as the fatigue failure point, and this can be computed for both controlled stress and strain loading conditions.

A rational fatigue failure criterion was developed at Arizona State University based on the Rowe and Bouldin's failure definition [25]. A new stiffness term (called stiffness degradation ratio) was defined by normalizing Rowe and Bouldin's parameter $n_i \times S_i$ by dividing it by the initial stiffness. Hence, Nf taken at the 50th cycle, was defined for both controlled strain and controlled stress modes as the number of load repetitions at the peak value of the stiffness degradation ratio-cycle number relationship. The results of Abojaradeh's method verified that 50% of the initial stiffness was the best value for the failure fatigue criterion.

Material properties undergo a progressive deterioration during fatigue tests, this phenomenon, along with premature failure, is deemed to be an effect of repeated loading. Specifically, as the number of cycles progresses, the norm of complex modulus decreases while phase angle increases. In stress-controlled tests, measured strain increases with the number of cycles until sample failure, while during strain-controlled tests the stress decreases with increasing number of cycles to values ideally near zero or until sample failure. In the classical method "WÖHLER" curve or fatigue curve, it is the relationship between the fatigue life (Nf) and the sample modulus reduction, Nf (50%) and the level of loading expressed by the initial strain (or stress) amplitude in a bi-logarithmic scale according to [53]. " ϵ_6 " is the strain level that leads to failure after one million cycles. The higher the value of " ϵ_6 " the higher the fatigue resistance of the asphalt mix. " ϵ_6 " and the complex (stiffness) modulus are used in some Empirical Mechanistic Pavement Design methods to determine the thickness of asphalt layers.

The “Département Génie Civil et Bâtiment” (DGCB) has developed the intrinsic damage approach that was used to determine the damage rate per loading cycle. One can utilize the DGCB approach, which was suggested by Di Benedetto, Soltani and Caverot (1996-1997). This method was initially proposed by [54] and validated and generalized by [28]. This method was further developed at the laboratory DGCB of ENTPE which defined the characteristics of 11 performed fatigue tests by using five different types of test geometry, which were adopted by different teams from Belgium (B), France (F), The Netherlands (N), Poland (PL), Portugal (P), Sweden (S) and United Kingdom (UK) as shown in detail in Table 2-1 [28], [54]–[56].

Table 2-1 Characteristics of various fatigue tests [57]

Type	Test Geometry	Type of loading/ Country of the team	Amplitude (10^{-6} m/m or MPa)
T/C		Tension-Compression « Homogeneous » F ₁ , S ₁	Strain : (80), 100, 140, 180 Stress : 0.9
2PB		Two Point Bending « Non Homogeneous » F ₂ , B ₁ , B ₂	Displacement; max strain: 140,180, 220 Load; max stress : 1.4
3PB		Three Point Bending « Non Homogeneous » N ₁	Displacement; max strain: 140,180, 220 Load; max stress : 1.4
4PB		Four Point Bending « Non Homogeneous » N ₂ , P, PL, UK	Displacement; max strain: 140,180, 220 Load; max stress : 1.4
IDT		Indirect Tensile Test « Non Homogeneous » S ₂	Load; max strain at first cycle: ~25, ~40, ~65

The failure does not always happen with the macroscopic fracture of the sample. Three different phases are identified during a fatigue test based on the analysis of experimental results as shown in Figure 2-9. Finding the true ratio of fatigue damage per cycle is the aim of this technique, specifically after the biased effects have been corrected.

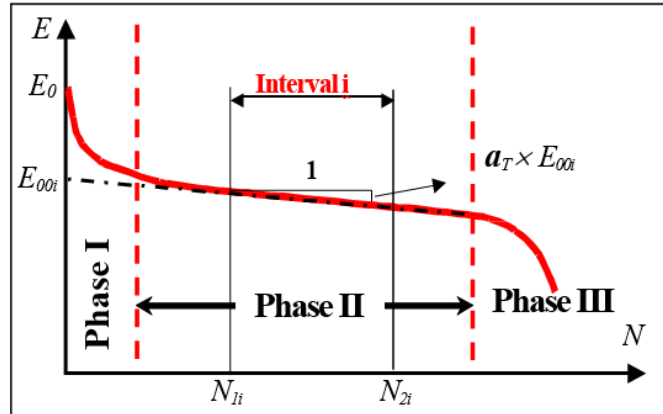


Figure 2-9 Determination of E_{00i} and a_T from the stiffness evolution curve [15]

Phase I (or adoption phase): fatigue alone cannot produce the rapid reduction in stiffness. Heating or thixotropy or another local phenomenon may play a significant role, and the reduction of the modulus can be recoverable. Artifact effects have full control of this phase if they are recoverable[15].

Phase II (or Quasi-stationary phase): this phase has minor bias effects, including thermal heating and thixotropy. However, the stiffness reduction is mostly controlled by the fatigue. With the DGCB approach, the fatigue damage development is studied in this phase. The bias effects are considered of second order and are calculated[15].

Phase III (or failure phase): at the end of this phase, a global failure occurs and the macro crack happens.

Everything has an initiation process that occurs in phase I and II, but a local propagation of crack(s) happens in phase III[15].

During the fatigue test, the dissipated energy per cycle increases in the stress control test as shown in Figure 2-10 while with strain control, it will be the opposite as shown Figure 2-11. Both of these conditions have influence on the stiffness of the sample, which will decrease. However, this value will be affected by dissipated energy variations. According to [58], stress control tests will increase the dissipated energy, causing heating of the sample that will lead to a decrease in the stiffness, whereas in the strain control test, a cooling phenomenon is noticed. The measured value of the stiffness is then higher than the real value. In other words, this phenomenon will affect the real fatigue life, and as a result, the stiffness value has to be corrected according to each case.

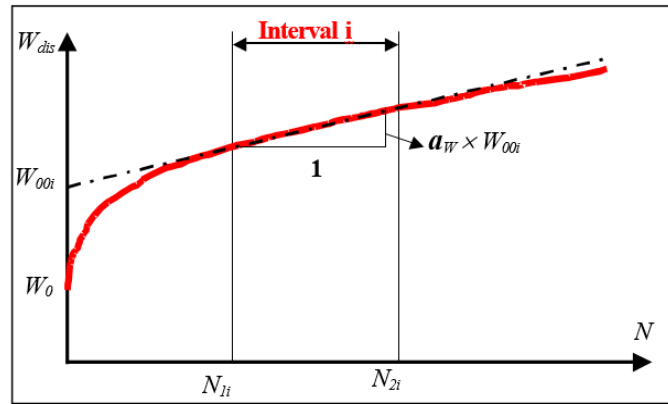


Figure 2-10 Determination of W_{00i} and a_w from the dissipated energy curve [15]

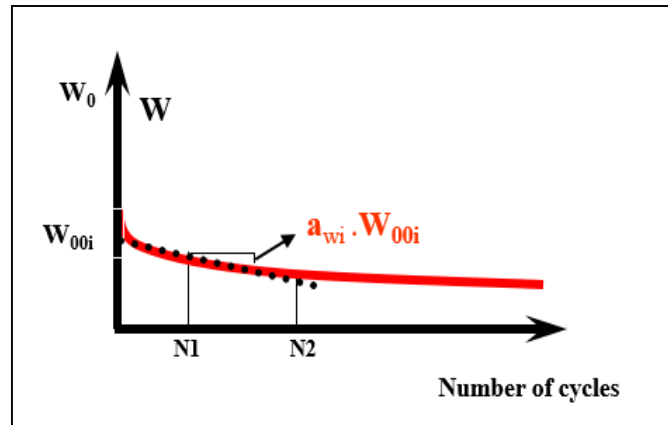


Figure 2-11 Determination of W_{00i} and a_w from the dissipated energy curve (Strain control) [59][15]

A linear evolution of the modulus “E” with number of cycles, is what this technique is based on during some specific periods. A noticeable progress is made due to a new global nonlinear approach [28].

2.2.4 Fatigue Test Methods

The fatigue resistance of asphalt mixtures is investigated both in-situ and in laboratories. The in-situ tests are generally done full-scale, by applying controlled traffic loads on instrumented pavement sections or using accelerated pavement facilities [60], [61], with the goal of evaluating material performances in real operating conditions. Laboratory tests investigate material properties in controlled conditions by monitoring the evolution of fundamental material properties under

repeated loading which are quite different from the in-situ tests. Standard laboratory tests include bending tests (2, 3 or 4 point respectively), shear tests and tension-compression tests. The results appear to be significantly affected by test type in laboratory tests on bituminous mixes [12]. For this reason, if test results have been obtained using different test configurations, the comparison of various materials in terms of their fatigue resistance can be misleading.

According to [20], fatigue behaviour of asphalt mixtures has been studied through various experimental assessments over the past decades. However, the prediction quality of fatigue life using any of these test methods are contingent on how well the assessment technique or test simulates the condition of loading, support, stress state, and the environment, in determining asphalt mix fatigue behaviour. Moreover, the availability and cost of equipment, in addition to ease of use are very important considerations for selecting any of these test methods as stated in NCHRP.

The major assessment methods employed for fatigue life evaluation of asphalt mixes are: Uniaxial Direct Tension, Uniaxial Tension Compression, Rotating Torsion, Compact Tension, Trapezoidal bending, 4-Point bending and indirect tensile test as shown in the Figure 2-12 [20].

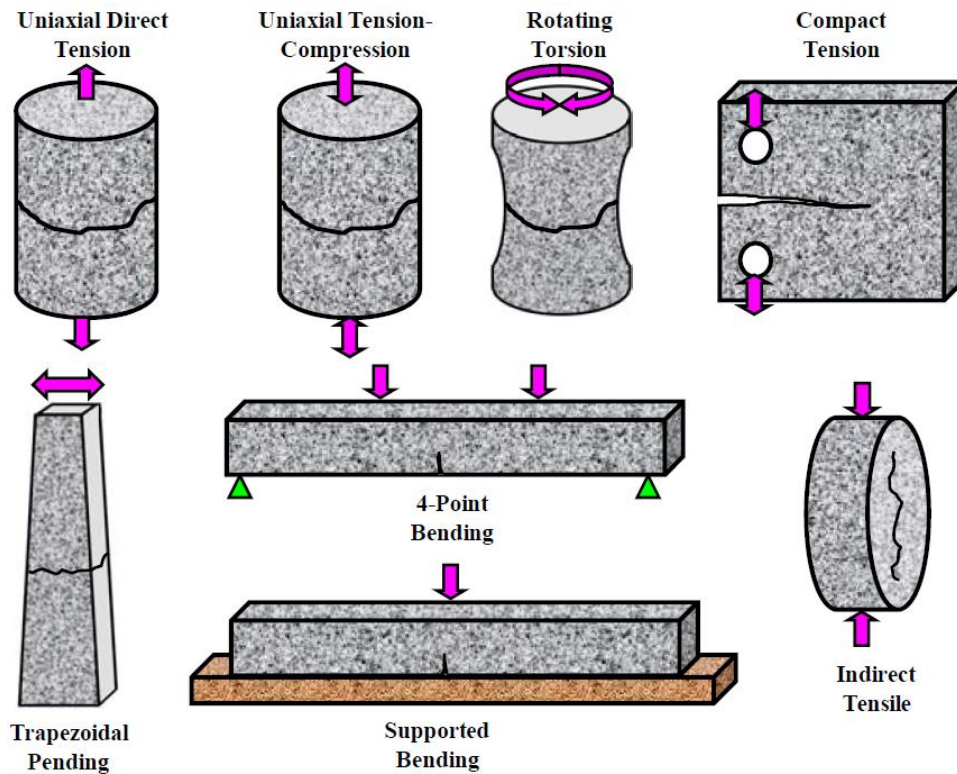


Figure 2-12 Commonly used fatigue test arrangements [20]

It should be noted that it is almost impossible for laboratory fatigue tests to completely simulate the actual field conditions, as there are a lot of field variables that are currently difficult to estimate or incorporate into laboratory testing simulation. Examples of this are random rest periods, multi-stress state and compound loading. As a result, there is often a variance in estimated fatigue life under field and laboratory conditions. To this anomaly in fatigue life into account, a shifting factor is considered in order to relate laboratory to field performance. The magnitude of the shift factor varies as it is based on certain factors such as asphalt layer thickness, traffic volume and composition, the mix properties, fatigue failure criterion, environmental conditions, and type of fatigue test [20].

2.2.4.1 Four-Point Bending Beam Fatigue (4PB)

The four-point bending beam fatigue (4PB) test was used to determine the fatigue life of different HMA mixtures due to the fact that it is the most popular North American test for the fatigue performance of asphalt mixtures [62].

The National Cooperative Highway Research Program (NCHRP) Report 9-57, which is responsible for a number of various laboratory fatigue cracking tests in terms of their field validation, recognized the 4PB test according to [63] is the best, based on bottom-up fatigue cracking and reflection cracking. Thus, the 4PB is considered to be the first option for the former and the third for the latter. In addition, the availability of test equipment is one of the advantages of 4PB [11]. The 4PB was compared to the Texas Overlay Test (OT) in reflective cracking, but the OT was better due to the better correlation between field and lab results. This outcome can be due to the fact that the 4PB is better than other tests in terms of variability; however, 4PB has shown a good sensitivity to the mix types. Moreover, 4PB is the best choice for bottom-up fatigue cracking evaluation and the second best in terms of its variability in linking the lab results and field performance. The second option regarding bottom-up fatigue cracking is the Semi-Circular Bend (SCB) test. Even though the SCB has good variability, the lab-to-field correlation is not as good as the 4PB [63]. The aforementioned characteristics of 4PB, such as ease of conducting the test, equipment availability, good correlation between lab and field results, and the popularity of the test, were the main reasons for choosing this test in this thesis. However, 4PB has some disadvantage, for example, non-homogeneous conditions in the samples and the poor assumption of linear elastic behaviour [12].

2.3 Polymer Modified Asphalt

Several studies indicate that asphalt modification can improve asphalt pavement performance and extend the service life of pavements. Table 2-1 shows different types of asphalt modification such as the use of additives, polymers, and chemical reaction modification. Among these different types of asphalt modification, using polymers is considered to be a common additive to modify asphalt, thus improving asphalt binder properties. Polymers can be incorporated into asphalt binders through either the direct addition of latex polymer to the asphalt, or the mixing and shearing of solid polymers during the addition process [64]. An inter-connecting matrix of polymers throughout the binder is created when the polymer is blended with asphalt binder [59]. This matrix gives a higher softening point, greater viscosity, greater elastic recovery, greater cohesive strength and greater ductility [65]. The increase in the viscosity of HMA mixes can improve rutting performance at high service temperatures [66]. Some researchers have stated that at low service temperatures, mixes with polymers can be affected by thermal cracking [67]. However, more studies reveal that polymer modification of the binder can improve the cracking resistance at low temperatures and can extend the fatigue life [68]–[72].

Researchers have found that the fatigue life of conventional asphalt mixtures were shorter than for the mixes with PMA. This happens because the polymer chain in asphalt caused a decrease in micro cracks. According to [73], various mixes have shown improvement in fatigue resistance, especially with SB (an in-situ cross-linked block copolymer), M SBS (modified SBS), and SBR (a linear random Styrene-butadiene latex polymer). In addition, the two polymers that had the most and the least impact on fatigue life were SBS and MCR (chemically modified experimental crumb rubber product), respectively.

The addition of polymers to the asphalt binder has allowed for the enhancement of asphalt mixture fatigue performance [15]. Nonetheless, there can be some difficulty with modification, due to the incompatibility of certain polymers and certain virgin binders at specific dosages, as was reported in the previous studies [64] [74]. Polymers modify the asphalt binder at the chemical and microstructural level [75] [76]. There are a number of factors that determine the success of the polymer modification, including the polymer content, the cross-linking agent and the method of

addition [77]. Polymers such as Styrene-Butadiene-Styrene have proven to be especially successful in improving asphalt properties in terms of fatigue life [3].

In addition, review of the literature on using the four-point flexural beam test for fatigue characterization of PMAC mixtures, indicates that the first phase in stiffness versus the number of cycles graph, was shorter for conventional asphalt mixtures, as compared to the PMAC mixtures. Also, it was reported that the stiffness of polymer modified mixes reduces relatively more, throughout the same phase. In the second phase of the fatigue curve, there was a substantial increase in the temperature of PMAC specimens during the test according to [78].

2.3.1 Types of Asphalt Modifications

Mineral fibers, rubbers and filler are examples of various modifiers that have been used in a large number of studies. In addition, pavement structure has been examined by many papers in terms of implementing different types of binder modifiers. Developments of asphalt modification involving natural and synthetic polymers were started as early as 1843 [79]. There are four popular asphalt modifiers that have been used in the asphalt industry, i.e. Crumb Rubber Modifier (CRM), Styrene-Butadiene-Styrene (SBS), Styrene-Butadiene-Rubber (SBR), and Elvaloy®.

There are many different kinds of polymers and additives as shown in Table 2-2, but a limited number are applicable for polymer modification. In case of a binder modification, a polymer must have the ability to decrease the level of degradation, especially at high temperatures, and to keep its properties in storage and handling within acceptable limits. Moreover, a suitable and economical balance with the binder should be achieved by the polymer and also, it should be able to handle traditional laying and being worked by mixing tools [80].

Table 2-2 Types of asphalt modifications [81]

	Type	Examples	
I.	Additive (excluding polymers) modification	1. Fillers	Lime, carbon black, fly ash
		2. Anti-stripping additives	Organic amines and amides
		3. Extenders	Lignin, sulfur
		5. Anti-oxidants	Zinc anti-oxidants, lead anti-oxidants, phenolics, and amines.
		5. Organo-metal compounds	Organo-manganese compounds, organo-cobalt compounds
		6. Others	Shale oil, Gilsonite, silicone, inorganic fibers
II.	Polymer modification	1. Plastics (a) Thermoplastics. (b) Thermosets.	Polyethylene (PE), Polypropylene (PP), Polyvinyl Chloride (PVC), PolyStyrene (PS), Ethylene Vinyl Acetate (EVA). Epoxy resins.
		2. Elastomers (a) Natural rubbers. (b) Synthetic rubbers.	Styrene-Butadiene Copolymer (SBR), Styrene-Butadiene-Styrene Copolymer (SBS), Ethylene-Propylene Diene Terpolymer (EPDM), Isobutene-Isoprene Copolymer (IIR).
		3. Reclaimed rubbers	
		4. Fibers	Polyester fibres, Polypropylene fibres
III.	Chemical reaction modification	Addition reaction (binder + monomer), Vulcanization (binder + sulfur), Nitration reaction (binder + nitric acid)	

Many researchers have investigated various modifiers as listed in the Table 2-1, and the advantages are shown in the Table 2-3 below:

Table 2-3 Benefits of various modifiers [82]

Modifier	Permanent Deformation	Thermal Cracking	Fatigue Cracking	Moisture Damage	Ageing
Elastomer	✓	✓	✓		✓
Plastomer	✓				
Tyre rubber		✓	✓		
Carbon black	✓				✓
Lime				✓	✓
Sulphur	✓				
Chemical modifier	✓				
Antioxidants					✓
Adhesion improvers				✓	✓
Hydrated lime				✓	✓

The most commonly used polymers for asphalt modifiers are Styrene-Butadiene-Styrene (SBS), Styrene Butadiene Rubber Latex (SBR), Polyethylene (PE), and Ethyl Vinyl Acetate (EVA) [83]. Styrene Butadiene Styrene (SBS) elastomers is the most widely used polymer when compared with the others. One SBS advantage is its ability to increase the elasticity of the asphalt [84], leading to better cracking resistance and better overall performance of the asphalt binder. SBS can also form an elastic network when mixed with the asphalt binder which will usually disappear at high temperatures and reform when the modified binder cools-down [85]. The formation of an SBS chain matrix acts as a reinforcement in the asphalt binder leading to an improvement in the permanent and recovered strains, compared to an unmodified binder [86]. Generally, using SBS will result in an increase in the production cost of asphalt which significantly restricts the broad use of SBS in road construction. However, to counter balance this cost, is its ability to reduce maintenance costs of the pavement during its service life [87].

In order for the modifiers to be efficient in terms of use and economics, they should have the following [88]:

- ease of availability,
- higher resistance of asphalt degradation at mixing temperature,
- ability to mix more simply with binder,
- more flexibility at lower pavement temperatures, and less deformation at high temperatures, and,
- be economical.

When the modifier is blended with the binder, the important features of the modifiers have to be kept in case of in-service uses and storage. In addition, the modifier has to keep its physical and chemical characteristics while it is stored, and stay in the base binder.

2.3.1.1 Elastomers

Thermoplastic elastomers are more highly desirable than plastomers in terms of binder modification because they are better at resisting permanent deformation as well as fatigue resistance. There are many examples of elastomers that are used for binder modification such as Natural Rubber (NR), Polyisoprene (IR), Isobutene Isoprene Copolymer (IIR), Polybutadiene (BR), Polychloroprene (CR), Styrenic Block Copolymers, and Styrene Butadiene Rubber (SBR). Among these examples, SBS copolymers and SIS copolymers are the most commonly used thermoplastic elastomers to modify the binder. A sequential operation of successive polymerization of Styrene-Butadiene-Styrene (SBS) or Styrene-Isoprene-Styrene (SIS) can form Styrenic Block Copolymers which are also known as Thermoplastic Rubbers (TR), since they combine the features of elastic and thermoplastic [89]. On the other hand, a reaction with a coupling and a successive polymerization of styrene and mid-block monomer has the ability to form a di-block precursor. As a result, multi-armed copolymers, also known as star-shaped, radial or branched copolymers, can be formed as well, not just linear copolymers. Figure 2-13 illustrates the structure of a SBS copolymer which has Styrene-Butadiene-Styrene tri-block chains composed of a matrix of Polybutadiene with a two-phase morphology of spherical PolyStyrene block domains.

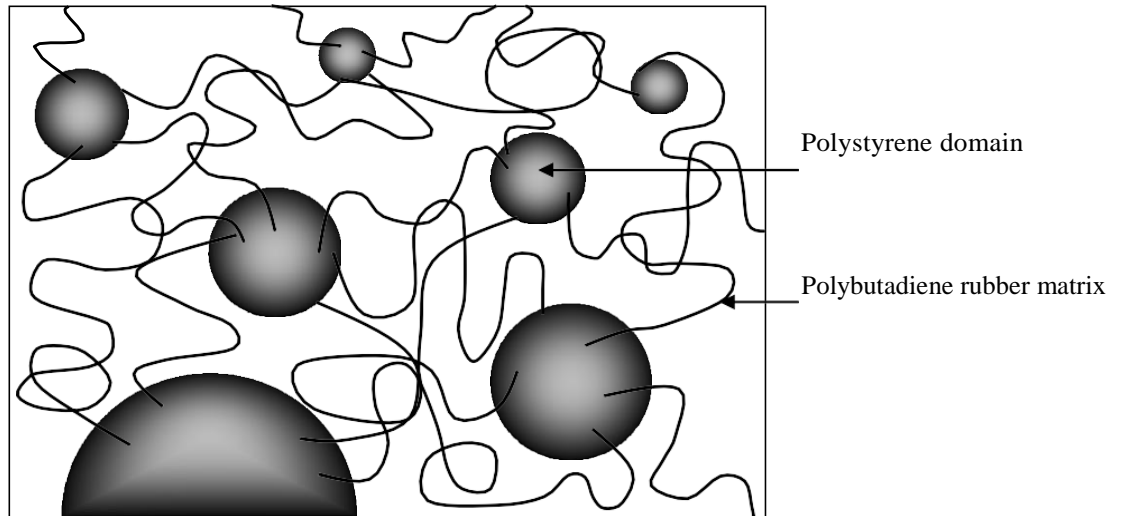


Figure 2-13 Schematic of a Styrene-Butadiene-Styrene (SBS) block copolymer [90]

The strength and elasticity of SBS copolymers are solely dependent on physical cross-linking of the molecules into a three-dimensional network. According to a number of studies [86], [91]–[93], Polyisoprene rubbery matrix mid-blocks have the ability to provide the binder material with remarkable elasticity or the strength of both polymer and Polybutadiene (PB) as given by the Polystyrene (PS) end-blocks. The Polystyrene domains in the matrix can be prevented by the chemical linkages between PS and PB blocks. Tg of PB blocks is around 80 °C, whereas Tg of PS blocks is around 95 °C. Although PB blocks are rubbery and they provide elasticity, PS blocks are glassy and they give the strength of SBS especially when the service temperatures of the paving binder are normal. Under the glass transition temperature of Polystyrene which is 100 °C, the efficiency decreases for cross-linkers; however, both the strength and elasticity are back to normal when the cooling starts in the Polystyrene domains as shown in Figure 2-14 (a-c) below.

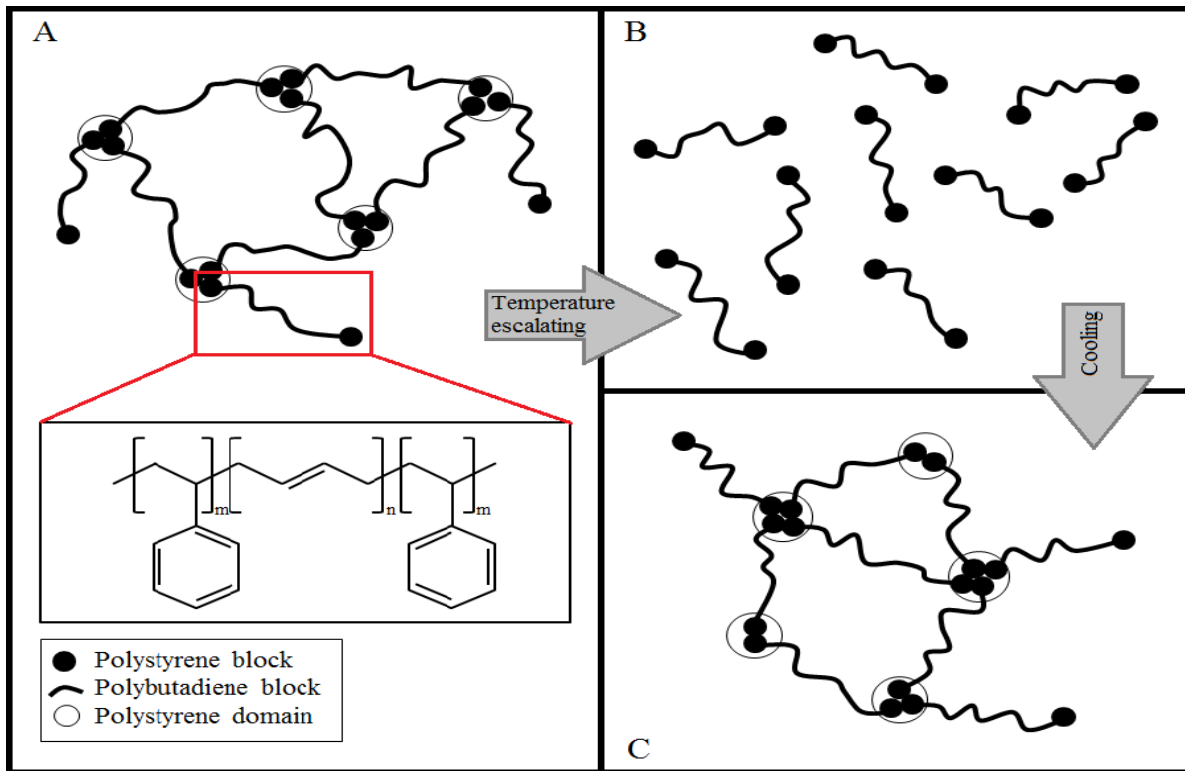


Figure 2-14 Structure of Styrene-Butadiene-Styrene (SBS) and schematic illustration of reversible crosslinks in SBS with the change in temperature [89]

2.4 Effect of Polymers on Fatigue

Since fatigue resistance is a very important factor in the development of high quality asphalt pavements, several studies have evaluated the effect of polymer-modified bitumens materials on such performance. For instance Lee et al., evaluated the fatigue behaviour of polymer-modified HMA using the small beam test with third-point loading at 15 °C [94]. The results showed that the polymer type, polymer dosage, asphalt source, aggregate type, and mix type have an effect on the characterization of the polymer-modified asphalt binders. For example, the high-temperature characteristics of asphalt binders were improved by increasing the polymer dosage. Although the SBR polymer was found to have better long-term aging characteristics than the SBS or C-polymer, the SBS and C-polymer showed more promising results in improving the fatigue characteristics of HMA. Ahmedzade et al., evaluated the fatigue resistance of SBS polymer-modified asphalt cement with different percentages 3%, 6%, and 9% SBS using the indirect tensile fatigue test (ITFT) [95].

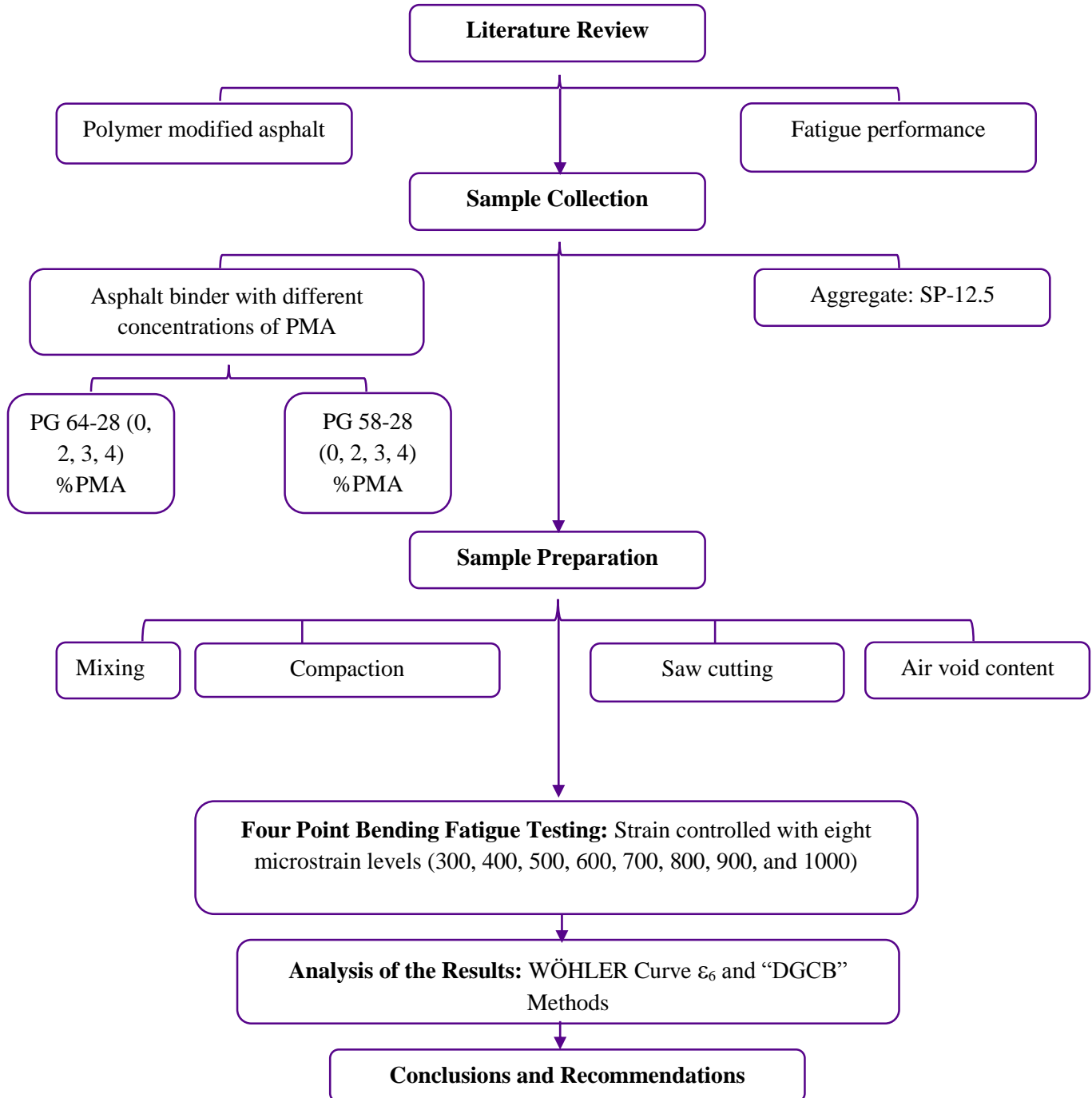
The results revealed that incorporating 6% of SBS resulted in the best fatigue behaviour at 25 °C. In another study, the fatigue properties of SBS modified mastic asphalt mixtures were analyzed using four-point bending beam fatigue tests and indirect strength tests. The results showed that crack resistance for SBS modified asphalt mixtures was significantly improved at 10 °C by a factor of 1.32 and 1.18 at 20 °C thereby, demonstrating a much higher fatigue life. The study also found that the roles that SBS modifiers had in retarding fatigue crack growth was more significant than crack initiation when the indirect tensile was conducted [96]. On the other hand, Kim et al found that SBS modifiers had the ability to reduce the rate of micro-damage accumulation resulting in an improvement in the cracking resistance of the SBS modified mixture compared to unmodified mixtures[97]. In another study, the fatigue performance of SBS modified mixes, at four different dosages of 3%, 5%, 7% and 10% by weight of the binder, was investigated based on the dissipated energy concept [98]. The author noticed that when more than 5% SBS modifier was used, the behaviour of the modified binders was similar to the modified binder with five percent. In the same manner, when less than 5% SBS modifier was used, the behaviour of the modified binders was similar to the unmodified binder. In conclusion, the results revealed that a significant improvement in fatigue behaviour was gained for all modified mixes when compared with the conventional mix [99].

Aglan studied the effect of three polymer modifiers, Styrene-Butadiene-Styrene (SBS) block copolymer, Ethylene Vinyl Acetate and Polyethylene, on the fracture and fatigue behaviour of asphalt mixture[100]. A four-point bending fatigue (4PB) beam test was performed under stress control at room temperature, 21.1 °C, using inverse haversine loading. The results showed that the strength and stiffness of asphalt pavement were increased by adding the three polymer modifiers and the asphalt mixture with SBS possesses higher flexibility and strength, which were desired for improving the performance of asphalt pavement [100].

Overall, adding SBS polymer to HMA has shown a great improvement in HMA performance in general and on fatigue performance in particular.

Chapter 3 METHODOLOGY

This flow chart explains the work of this thesis showing the literature review and the experimental work:



3.1 Materials Properties and Sample Preparation

3.1.1 Asphalt Cement Properties

The asphalt cement used in the study is mostly sourced from western crude and PG graded at 58-28 and 64-28. These two sources represent asphalt sold by Yellowline Asphalt Products Ltd., but are not typically used to produce PMAs. The samples were taken either from tanks at the terminal or directly from rail cars sent from the supplier. The PG 64-28 is a neat blend prepared at the terminal and mixed in the storage tank. All samples were taken at the same time to ensure consistency.

The asphalt cement properties of each binder can be found in Table 3-1. Each binder was tested at the appropriate test temperatures as designed by AASHTO. It was determined that both binders meet AASHTO M320 requirements prior to modification. Additionally, the ash content was tested to show that each asphalt cement meets OPSS requirements. They were blended using the same source of SBS and at concentrations of 0, 2, 3, and 4 percent to produce a total of 8 different binders.

Asphalt cement was characterized per AASHTO T315 to determine the effect of polymer on the modulus at the high-performance grade temperature on the DSR. AASHTO T313 testing on the BBR was used to characterize the low temperature properties. Each PMAC was tested via the low temperature grade taken from the source binder [101].

Table 3-1 Properties of asphalt cement used in PMA preparation [101]

Property	Test Method	PG 64-28	PG 58-28
Original Material			
Ash Content, %	ASTM D2939-09	0.04	0.03
Viscosity (Pa.s), At 135°C	AASTHO T316	0.374	0.266
$G^*/\sin(\delta)$, kPa	AASTHO T315	1.12	1.18
RTFO Residue¹	AASTHO T240		
Mass Loss (%)	AASTHO T240	0.45	0.37
$G^*/\sin(\delta)$, kPa	AASHTO T315	2.58	3.05
PAV Residue²	AASHTO R18		
$G^*\sin(\delta)$, kPa	AASHTO T315	3980	3550
m-Value At Pass Temperature	AASHTO T313	0.310	0.358
Stiffness, MPa At Pass Temperature	AASHTO T313	282	187
m-Value At Fail Temperature	AASHTO T313	0.257	0.294
Stiffness, MPa At Fail Temperature	AASHTO T313	579	385
True Grade	AASHTO M320	65.0-28.4	59.4-31.4

¹ RTFO is Rolling Thin Film Oven

² PAV is Pressure Aging Vessel.

3.1.1 SBS Polymers

The SBS polymer has a Styrene content of 31.1% and SBS B has a Styrene content of 31.6%. However, in this thesis only SBS A was used. Figure 3-1 shows the sample image of Styrene-Butadiene-Styrene (SBS A).



Figure 3-1 Sample of SBS A

3.1.2 Blending

The asphalt cement was blended using the same methodology as in[101]. The process was completed using a Silverson high shear mixer and heating mantle. After preheating the asphalt cement to 170 °C, polymer was added and milled for one hour. A crosslinking agent was added at the end of the hour and allowed to mill for a further 30 minutes. The crosslinking agent was added at 10% by weight of the polymer. After milling the crosslinking agent and polymer, the high shear mill speed was reduced, and the sample was milled for another hour. The final hour was used as a curing time. Temperatures were monitored and maintained at 180 °C ± 5 °C. This method produced PMAC that compared well with production batches [101].

3.2 Bending Beam Testing Matrix

The 4PB testing was done using a Superpave 12.5 FC2 mix design produced by Aecon Materials Engineering. The mixes were prepared for all of the eight binders.

3.2.1 Asphalt Mixtures

A Superpave 12.5 FC2 mix was selected due its good field performance observed by Aecon Construction. The mix design was prepared by Aecon Materials Engineering³. Figure 3-2 also shows Aggregate 1, 2, 3 and 4 as used in the study. Gradation of the aggregate blend and asphalt cement percentage can be found in Table 3-3.

Table 3-2 Gradation and volumetric properties of aggregates

AGGREGATE DATA	AGG. SPECIFIC GRAVITY	AGG. ABSORP. (%)	AGGREGATE GRADING - PERCENT PASSING												
			37.5	25	19.0	16.0	12.5	9.5	4.75	2.36	1.18	600	300	150	75
AGG #1	2.883	0.4	100.0	100.0	100.0	100.0	90.5	62.0	4.0	1.0	1.0	0.9	0.9	0.8	0.8
AGG #2	2.945	0.6						100.0	80.6	20.0	8.6	5.4	4.0	3.3	2.7
AGG #3	2.926	0.7						100.0	99.8	92.0	56.5	34.0	18.5	9.5	5.0
AGG #4	2.918	0.6						100.0	96.5	66.5	44.0	31.5	22.0	16.3	11.5
AGG #5															
AGG #6															
Coarse Agg. Gsb	2.892		Fine Agg. Gsb				2.915		Combined Gsb			2.905			

*JMF Adjusted to Allow for 2.0 % Fines Returned to the Mix

³ Superpave Mix Design Report in Appendix



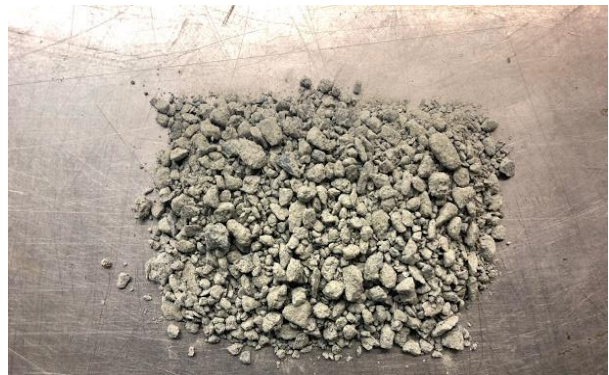
(i) Aggregate 1: HL 1 Stone



(ii) Aggregate 2: Chip



(iii) Aggregate 3: Washed DFC Fines



(iv) Aggregate 4: Screenings

Figure 3-2 Images of aggregate material composition

Table 3-3 Asphalt mix formula

Job Mix Formula- Gradation Percent Passing *														
%AC	37.5	25	19.0	16.0	12.5	9.5	6.7	4.75	2.36	1.18	600	300	150	75
5.20	100	100	100	100	96.0	84.0		56.4	40.4	25.8	17.3	11.4	7.8	5.5

The asphalt cement content of the mix has been set at 5.20% [101] . Table 3-1 contains the relevant mix design data. The mixes were prepared for both binders. For neat asphalt, mixing and compaction temperatures were determined using the equiviscous method described by AASHTO T312. PMA mixing and compaction temperatures were chosen by comparing Yellowline products to the PMAC, with the PMA temperatures being higher to account for the increased stiffness of

the binder [62]. Depending on the viscosity of the binder, the mixing and compaction temperatures for each AC were provided by the Yellowline Company as follows in Table 3-4 below:

Table 3-4 Mixing and compaction temperatures

Performance Grade (PG)	Mixing Temperature °C	Compaction Temperature °C
58-28 0% SBS	149	137
64-28 0% SBS	153	142
58-28 2, 3, 4% SBS	160	150
64-28 2, 3, 4% SBS	160	150

The asphalt was compacted using a PReSBOX® Shear Compactor as shown in the Figure 3-3 to form an asphalt slab. After compaction, 380L×63W×50H mm beam specimens were cut using a diamond saw as shown in Figure 3-4 and the air voids of the samples checked to make sure they were in the 7±1% range.



Figure 3-3 PReSBOX® Shear Compactor at the CPATT Lab, University of Waterloo

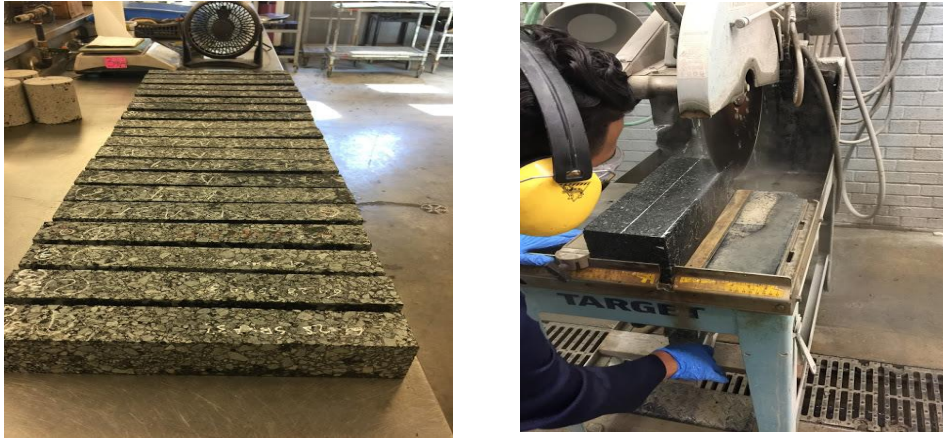


Figure 3-4 The use of diamond saw for asphalt mix cutting and 380L×63W×50H mm beam specimens. Eight (8) HMA samples of 0%, 2%, 3%, and 4% of SBS A were produced through the process described in Figures 3-3 and 3-4, for performance grade PG 64-28 and PG 58-28 respectively making a total of 32 rectangular sizes of HMA samples. However, for PG 58-28 four samples of 0%, 2%, 3%, and 4% of SBS A with 16 specimens in total, were tested at different strain levels.

3.2.2 Asphalt Mixture Volumetric Properties

The hot mix asphalt samples used in this study were composed of aggregates and asphalt cement with incremental percentages of Styrene Butadiene Styrene (SBS) from 0%, 2%, 3% and 4%. Two types of asphalt cement, i.e., Performance Grade of 64-28 and 58-28, were modified in this manner. As shown in Figure 3-5 the air voids for these HMA samples were calculated after estimating sample's Specific Bulk Gravity (G_{mb}) and Theoretical Maximum Specific Gravity (G_{mm}) using AASHTO T 166: Bulk Specific Gravity of Compacted Asphalt Mixtures Using Saturated Surface-Dry Specimens and AASHTO T 209: Theoretical Maximum Specific Gravity and Density of Bituminous Paving Mixtures, respectively. The maximum relative density (MRD) for this mix design was found to be 2.673. Air void percentage was specified to be within the range of $7\pm 1\%$.

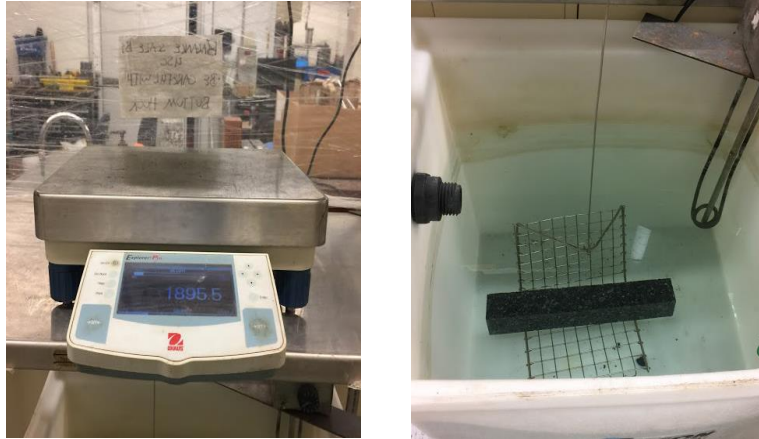


Figure 3-5 Bulk relative density (BRD) determination by (AASHTO T 166 2007a)

$$G_{mb} = \frac{A}{(B - C)}$$

Where,

Specific Bulk Gravity (G_{mb})

A = Mass of sample in air (g)

B = Mass of saturated surface dry (SSD) sample in air (g)

C = Mass of sample in water at 25 °C (g)

$$G_{mm} = \frac{A}{(A - C)}$$

Where,

Maximum Specific Gravity (G_{mm})

A = Sample mass in air (g)

C = Mass of water displaced by the sample (g)

$$\text{Air void (\%)} = \frac{G_{mm} - G_{mb}}{G_{mm}}$$

With respect to the mix design properties, AME Company provided Superpave™ mix design as shown below in Table 3-6 and this specification was guided by the volumetric design procedure. Description of the design variables are as shown below.

Where,

N_{de} = Estimated compaction after indicated amount of traffic, ESAL (Typical Min Air Void = 11%)

N_{ini} = Compaction during construction (Typical Design Air Voids = 4%)

N_{max} = Long term compaction under traffic (Typical Maximum Air Voids = 2%)

Voids in Mineral Aggregates, VMA (%) is the volume concentration of inter-granular void space in a compacted mix space occupied by asphalt. It is therefore a percentage by volume of the total asphalt mix.

$$VMA = 100 - \frac{G_{mb} P_s}{G_{sb}}$$

VMA = V effective asphalt + V air voids

G_{mb} = Bulk specific gravity of the aggregate

P_s = Aggregate content by weight of mix (%)

G_{sb} = Bulk specific gravity of the aggregate

Voids filled with asphalt, VFA % is the percentage of VMA that is filled with asphalt.

$$VFA = 100 \times \frac{VMA - V_a}{VMA}$$

V_a = Volume of air voids

VMA = Voids in mineral aggregates

Table 3-5 HMA mix design properties

Property	Specifications	Design
Air Voids, %, (At N_{des})	3.5 ± 0.3	3.8
% G_{mm} at N_{des} ,	96.5 ± 0.3	96.2
% G_{mm} at N_{ini}	89 Max	87.3
% G_{mm} at N_{max} ,	98 Max	97.1
Voids in Mineral Aggregate (VMA), %	14 Min	16.1
Voids Filled with Asphalt (VFA), %	65 – 78	76.2
Dust Proportion (DP)	0.6 – 1.2	1.1
Tensile Strength Ratio (TSR), %	80% Min	94.1

3.3 Testing Regime

3.3.1 4PB Test

The 4-point bending beam fatigue test was carried out in accordance with the AASHTO T 321 [8] procedure “*Method for Determining the Fatigue Life of Compacted Hot-Mix Asphalt (HMA) Subjected to Repeated Flexural Bending*”. The test is entirely computer-controlled consisting of a load frame, a closed-loop control, and data acquisition system [62], as shown in Figure 3-6.

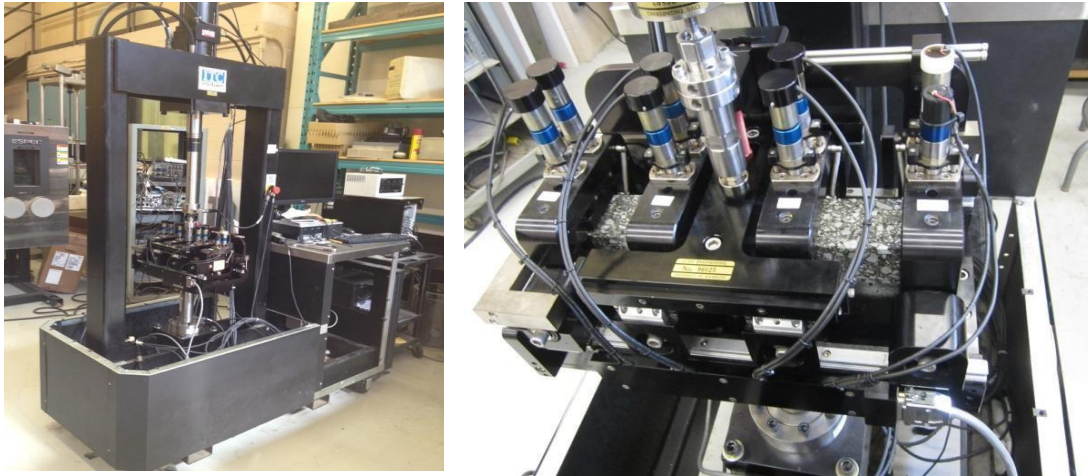


Figure 3-6 4PB and Sample set up at the University of Waterloo

Beam specimens of 380L×63W×50H mm were conditioned for 2 hours at the test temperature of 20 °C to achieve a homogeneous temperature throughout the sample, in a four-point bending frame, where they are subjected to repeat cycles of flexural sinusoidal loading at a frequency of 10 Hz. The test was conducted until the initial modulus was reduced to at least 50% of the initial stiffness. The initial load to deflection value (K^*) was estimated by applying 50 load cycles at a constant strain level. The test continued until the K^* was at 50% of the initial value, at which the test stopped and the number of cycles was recorded as the fatigue life $N_{f50\%}$. All of the asphalt mixture samples were tested at 700 $\mu\text{m/m}$ and the range of the strain levels was at 300, 400, 500, 600, 700, 800, 900 and 1000 $\mu\text{m/m}$ depending on the results that led to finding the " ϵ_6 ". After that, all the maximum tensile stresses and strains of samples were calculated by using the following equations:

$$\sigma_t = \frac{0.357 \cdot P}{b \cdot h^2} \quad (1)$$

$$\epsilon_t = \frac{12 \cdot \delta \cdot h}{3 \cdot L^2 - 4 \cdot a^2} \quad (2)$$

where,

σ_t = Maximum peak – to – peak stress, MPa,

ϵ_t = Maximum peak – to – peak strain, m/m,

P = Peak – to – peak load applied by actuator, N;

b = Average specimen width, m,

h = Average specimen height, m,

δ = Maximum deflection at the center of the beam, m;

L = Length of the specimen, 0.357 m,

a = Length between the clamps ($L/3 = 0.119$ m)

In addition, the flexural stiffness, phase angle, and dissipated energy were also determined as follows:

$$S = \frac{\sigma t}{\epsilon t} \quad (3)$$

$$\phi = 360 \cdot f \cdot s \quad (4)$$

$$D = \pi \cdot \sigma t \cdot \epsilon t \cdot \sin(\phi) \quad (5)$$

where,

S = Stiffness Modulus, Pa,

ϕ = Phase angle, degrees,

f = Load frequency, Hz,

s = Time lag between P_{\max} and δ_{\max} , seconds,

D = Dissipated energy per cycle, J/m³

3.4 Fatigue Analysis

Two different approaches were used in this project in order to evaluate the fatigue characterization with the 4PB test:

- Traditional Method: analysis of the tests with the criteria of fatigue failure $Nf_{50\%}$ WÖHLER curve.[103]

- ‘Newer’ Method Developed at École Nationale des Travaux Publics de l’État (ENTPE) in Lyon, France: analysis of fatigue tests in terms of damage rate "DGCB" method.

3.4.1 Traditional Method

Multiple criteria have been used in order to characterize the fatigue failure of the asphalt mixes. The classical fatigue failure is the number of cycles N of the sample, leads to failure at the certain levels of loading. This criterion depends on the stiffness to be reached at half of the initial stiffness value of K^* (E_0) based on [104][105][13].

This criterion is used with the WÖHLER curve or fatigue curve as shown in the Figure 3-7, showing that the relation between the fatigue life (N_f) the sample modulus reduction, $N_{f_{50\%}}$ and the level of loading expressed by the initial strain (or stress) amplitude in a bi-logarithmic scale according to [53]. Moreover, given a number of strain amplitudes, the " ϵ_6 " failure at 1,000,000 cycles can be determined based on the curve as well. However, the amplitude for 1 million cycles " ϵ_6 ", do not give a complete picture of fatigue performance because they are arbitrarily decided ‘limits’ and are therefore susceptible to misinterpretation [12]

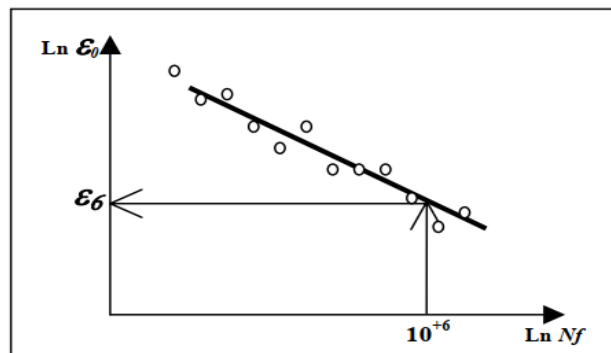


Figure 3-7 WÖHLER (or fatigue) curve and determination of " ϵ_6 " [15].

Although they are widely used, standard asphalt mixture fatigue tests, such as the four-point bending beam test described above (AASHTO T 321) and shown in Figure 3-8, are inherently variable. In such tests, the loading changes over the length of the sample, due to the loading conditions, and over the term of the test, due to the changing properties of the sample from the fatigue loading. Due to the non-homogeneity of the 4PB test, the inconsistency of results produced have been shown as indicated in Figure 3-8 [15]. The work of a number of researchers, notably of

Di Benedetto and his group, have shown that tension-compression fatigue testing with homogenous loading provides a more consistent method to test fatigue [12], which will be the subject of a thesis that follows the current one.

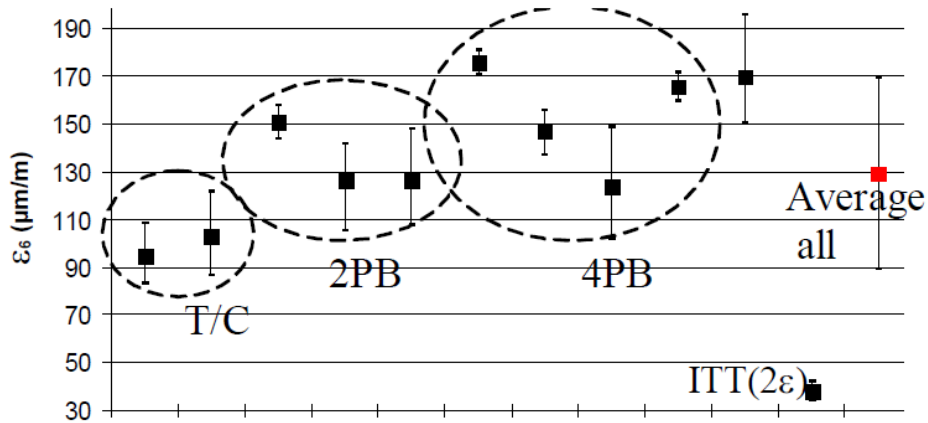


Figure 3-8 Strain amplitudes " ϵ_6 " giving failure at 1 000 000 cycles from the 11 fatigue tests including the 4-point bending beam (4PB) [12]

3.4.2 Damage Analysis "DGBC"

Standard parameters such as the number of cycles to 50% modulus reduction, $N_{f50\%}$, and the amplitude for 1 million cycles, " ϵ_6 ", do not present a complete picture of fatigue performance because they have arbitrarily decided 'limits' and are therefore susceptible to misinterpretation [12]. More complete approaches are needed to be implemented in order to aid the interpretation of fatigue results such as those previously discussed, based on damage rate, along with methods to filter bias effects such as thermal heating and thixotropy (reduction in viscosity from loading) [15]. Improved understanding of the fatigue performance of PMA mixtures could then be used to develop models that can predict the fatigue performance based on the polymer type and content, which would prove to be extremely valuable to the development of high performance roads.

Département Génie Civil et Bâtiment "DGCB" has devolved the intrinsic damage approach that used to determine the damage rate per loading cycle. One can utilize the DGCB approach, which was suggested by Di Benedetto, Ashyer Soltani and Caverot in their 1996-1997 research. This method initially was proposed by the work of Soltani (1998) and validated and generalized by Baaj (2002).

The equations below are used to calculate the damage rate per loading cycle.

D_{exp} = Represents the experimental damage parameter which has been corrected from the artifact effects and shown in the equation below:

$$D_{exp} = 1 - \frac{E_0 - E_N}{E_0} \quad (6)$$

E_0 = The initial modulus (at the beginning of the test) as shown in Figure 2-9.

E_N = The current cyclic stiffness

There are four periods:

- Interval $i = -1$ from 30000 to 60000 cycles.
- Interval $i = 0$ from 40000 to 80000 cycles.
- Interval $i = 1$ from 50000 to 150000 cycles.
- Interval $i = 2$ from 150000 to 300000 cycles.

Not all periods can always be taken into account since these periods have to be in phase II. In each quasi-linear period, the number of cycles is the only notable change in modulus. The development is defined next by a linear regression as shown in Figure 2-9. A linear regression extrapolation at the first cycle determines E_{00i} , which is the initial stiffness for the period i ($i = -1, 0, 1$ or 2) in Figure 2-9. The experimental damage slope is represented by a_T and equals the slope of the regression line of $|E^*|$ in the period (i) divided by E_{00i} for the same period ($a_T = D_{exp}E_0/E_{00i}$).

a_T = Represents different values based in the selected interval because of the irregularity of damage. The experimental damage slope for each period has two different elements:

$$a_T = a_F + a_B \quad (7)$$

Where a_F represents the true fatigue slope, and a_B is the slope of the dissipated energy per cycle, for the same period. Based on some mathematical and experimental calculations, the artifact effects evolve in proportion to the change in the dispersed energy led by either a positive or a negative effect. The fatigue slope a_F is calculated according to the following proposed equation:

$$a_F = a_T + a_W \frac{C_i \cdot (E_0 - E_{00i})}{E_{00i}} \quad (8)$$

A linear extrapolation at the first cycle of loading, as depicted in Figure 2-10 and 2-11, determines the value W_{00i} of the dissipated energy, normalizing the slope of the dissipated energy per cycle curve a_W for the specific period. In phase II, the nonlinear damage evolution is mainly considered

by a coefficient C_i and this coefficient has the following values: $5/6$, $4/5$, $3/4$ and $2/3$ for $i = -1, 0, 1$ and 2 , respectively.

The value of a_F is dependent on the selected period, whereas the fatigue law is linear by period; thus, the damage evolution is non-linear.

In this project, the DGCB method was utilised by using strain control with the four-point bending test machine. Because of the failure conditions $Nf_{50\%}$ reduction of the initial stiffness, there is no way to find phase III during the fatigue failure test in this project. It was noticed that the dissipated energy during the fatigue test was decreased, however using the phase II quasilinear phase, the bias effects were not as strong as in phase one. Nonetheless, they still need to be considered in the calculations for fatigue damage characterization purposes. In order to eliminate or isolate this bias effect four intervals were used, as shown below:

- Interval $i = 1$ from 30000 to 60000 cycles.
- Interval $i = 2$ from 40000 to 80000 cycles.
- Interval $i = 3$ from 50000 to 150000 cycles.
- Interval $i = 4$ from 150000 to 300000 cycles.

Chapter 4 RESULTS AND DISCUSSION

4.1 Tests Parameters

The equations mentioned in the methodology chapter based on the AASHTO T 321 procedure, were used to calculate the maximum tensile stress and strain of each sample as well as, the flexural stiffness, phase angle, and dissipated energy, which were calculated to represent the fatigue test. In these graphs, the test conditions were fixed as indicated in Table 4-1 in order to evaluate the fatigue life under the same conditions.

Table 4-1 Test conditions

Test Parameter	Test Conditions
Temperature (°C)	20
Loading frequency (Hz)	10
Mode of loading	Load cycles at a constant strain level
Strain amplitude ($\mu\text{m}/\text{m}$)	700
Failure conditions	50% reduction of the initial stiffness value ($K=\text{Load}/\text{Deflection}$)

4.1.1 Stiffness (K^*)

The stiffness value K^* was taken as the applied load over the measured vertical deflection at the centre, without taking into account sample geometry. The desired maximum deflection value was calculated based on the desired strain. For example, for a strain of 700 $\mu\text{m}/\text{m}$, the displacement was -0.385 mm, with the negative value indicating that the deflection occurred downward. During the test, the deflection did not stay constant, so the results had to be corrected based on the actual maximum deflection.

Figure 4-1 shows the evolution of the normalized stiffness (K^*/K_0^*) versus the number of cycles $N_{f50\%}$. The results illustrate a clear influence on the fatigue lifespan by increasing the concentration of polymer. For PG 58-28, the results show better fatigue life with polymer modified asphalt, as

well as with the PG 64-28 in terms of the number of the cycles $Nf_{50\%}$. For example, PG 58-28 SBS A 4%, at the same test conditions, reached 1130383 cycles while PG 64-28 SBS A 4% reached 194524 cycles as shown in Figure 4-2.

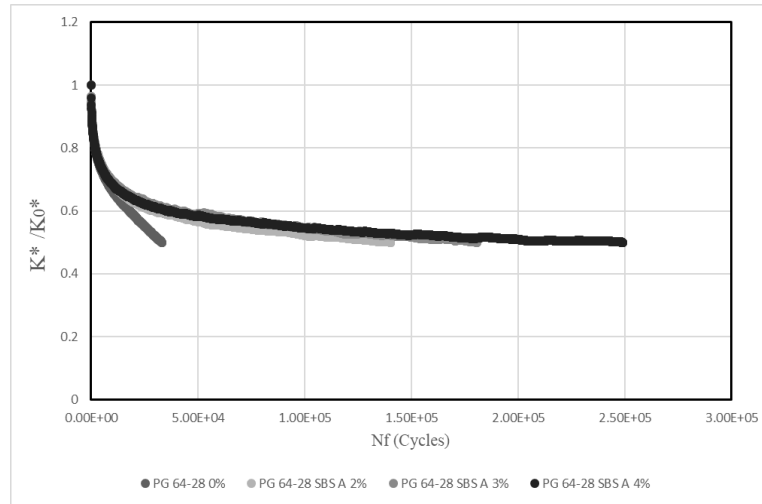


Figure 4-1 K^*/K_0^* versus $Nf_{50\%}$ at 700 $\mu\text{m/m}$ PG 64-28

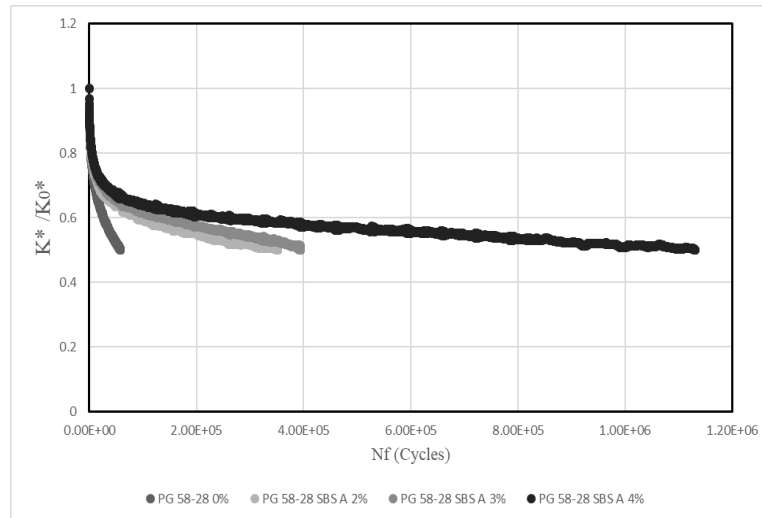


Figure 4-2 K^*/K_0^* versus $Nf_{50\%}$ at 700 $\mu\text{m/m}$ PG 58-28

4.1.2 Stiffness Modulus (E^*)

Figures 4-3 and 4-4 illustrate the normalized stiffness modulus (E^*/E_0^*). E^* are calculated by taking the stress divided by the strain, taking into account each sample geometry (height x width). The results for PG 64-28 and PG 58-28 show that the unmodified asphalt mixes reached the 50% reduction failure very quickly, while, by adding SBS A polymer 2%, 3%, and 4% improved the fatigue life resistance considerably. Note that the softer binder PG 58-28 had better fatigue resistance by adding polymer than stiffer binder PG 64-28 in this project.

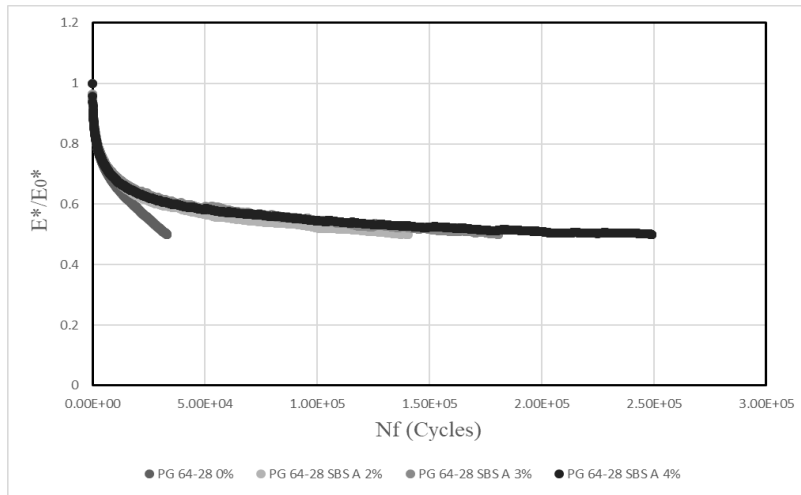


Figure 4-3 E^*/E_0^* versus $Nf_{50\%}$ at 700 $\mu\text{m/m}$ PG 64-28

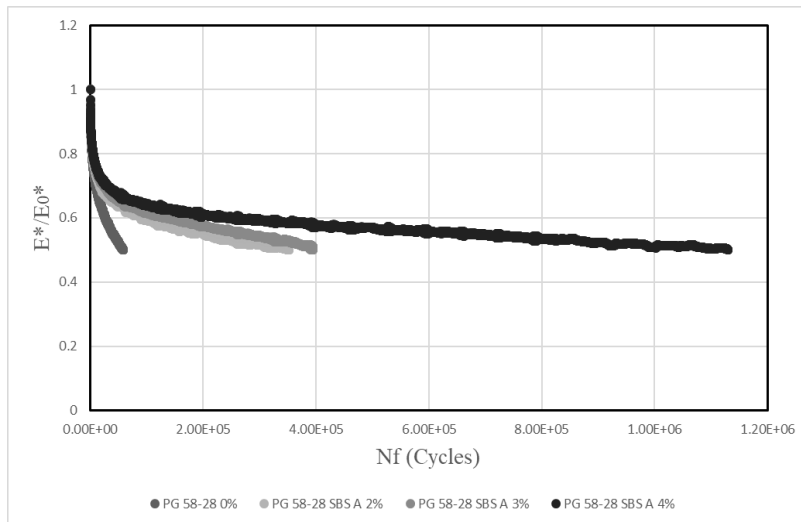


Figure 4-4 E^*/E_0^* versus $Nf_{50\%}$ at 700 $\mu\text{m/m}$ PG 58-28

Figure 4-5 illustrates the initial stiffness (K^*) and stiffness modulus (E^*) for both mixes PG 58-28 and PG 64-28 versus the polymer content at 700 $\mu\text{m/m}$ strain amplitude. It shows how the tolerance range ($\pm 6\text{mm}$) in AASHTO T 312 for the 4PB test sample dimensions have a significant effect on fatigue characterization when the results are corrected by taking sample dimensions into account for E^* values. This indicates that these considerations have to be, at minimum, taken into account when conducting fatigue tests. Additionally, it shows that the initial stiffness is influenced more by the base binder than the polymer content.

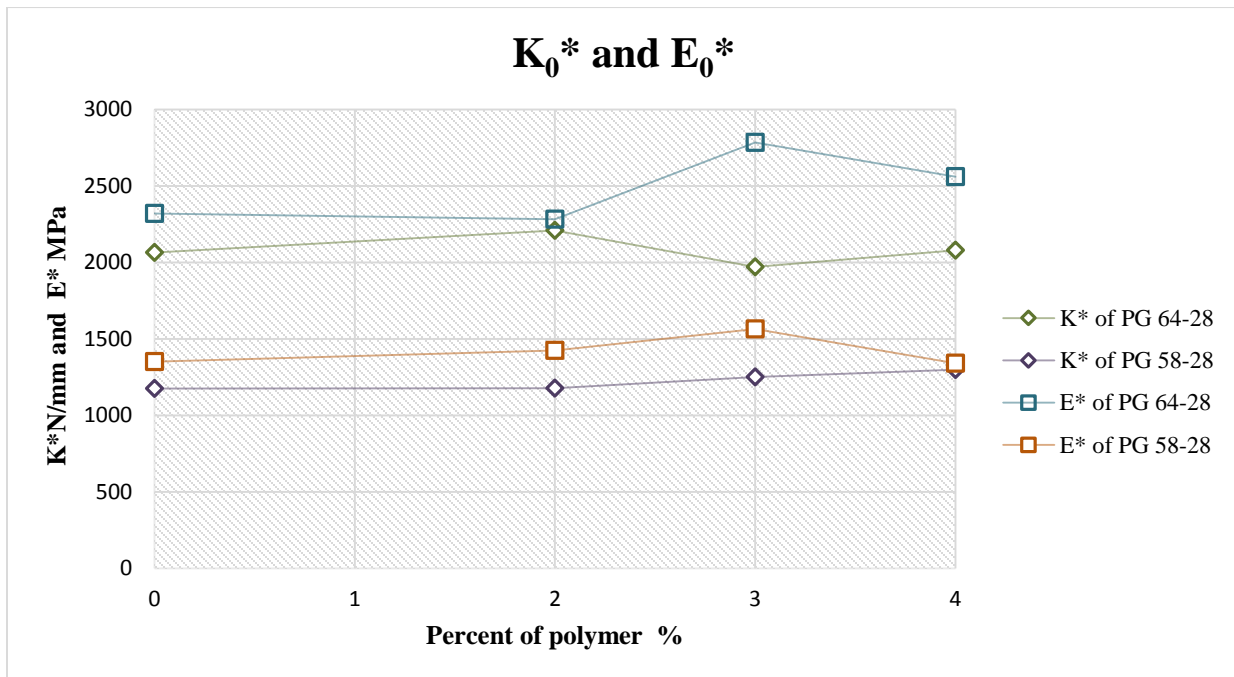


Figure 4-5 K^* and E^* for PG 58-28 and PG 64-28 versus present of polymer at 700 $\mu\text{m/m}$

4.1.1 Actual Strain Level

In addition to the dimensions of the sample affecting the Stiffness Modulus, these dimensions also had an influence on the actual applied strain level of the samples. The applied displacement was calculated based on sample dimensions of 380L \times 63W \times 50H mm ($\pm 6\text{mm}$) while the actual dimensions differed after cutting, as mentioned. The actual displacement also differed from the displacement input into the system, therefore the actual strain values needed to be corrected based on the actual dimensions and displacement values for each sample. Overall, the differences in the

actual dimensions, also have a significant impact on the results of the actual strain as indicated in Table 4-2.

Table 4-2 The desired and actual stain levels

Sample	Desired Strain	Actual Strain	Sample	Desired Strain	Actual Strain
PG 58-28	µm/m	µm/m	PG 64-28	µm/m	µm/m
0%	300	302	0%	300	279
	400	414		400	409
	500	512		400	409
	700	744		500	528
				500	543
SBS A 2%	500	515		700	724
	600	608		700	718
	700	723			
	1000	1104	SBS A 2%	400	408
				400	411
SBS A 3%	600	635		500	551
	700	718		500	562
	800	847		500	544
	1000	1132		700	773
				700	778
SBS A 4%	700	769		700	698
	800	817			
	900	885	SBS A 3%	400	433
	1000	965		500	522
				500	529
				700	694
				700	693
			SBS A 4%	500	612
				500	537
				600	654
				600	644
				700	725
				700	755
				1000	1050

4.1.2 Phase Angle (δ)

The phase angle (δ) versus the number of cycles $Nf_{50\%}$ is plotted in Figures 4-6 and 4-7. When the stiffness is increased, the phase angle generally decreases, as the material is considered more elastic. As mentioned, the benefit of adding SBS polymer is increased elasticity, thus increased stiffness in the mixture can be expected. It is visible from Figures 4-6 and 4-7 that the unmodified asphalt mix has a higher phase angle. On the other hand, the polymer modified asphalt with 2%, 3%, and 4 %, respectively, has a lower phase angle because it tends to be more elastic due to the polymer addition.

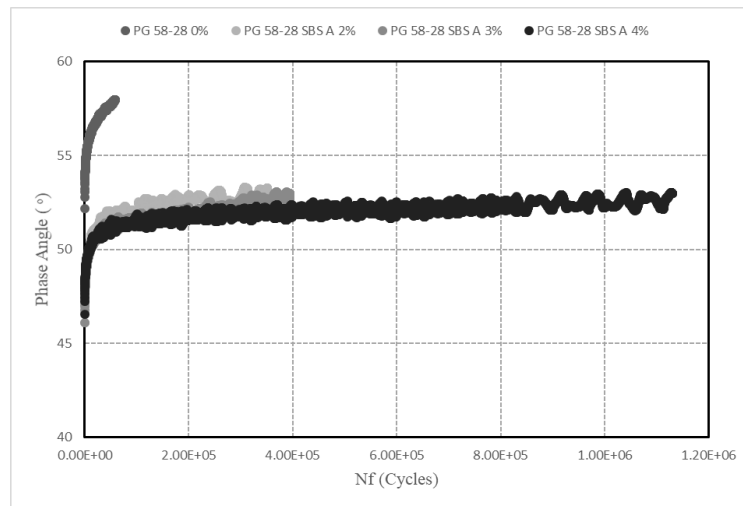


Figure 4-6 Phase Angle δ (°) Versus $Nf_{50\%}$ at 700 $\mu\text{m/m}$ PG 58-28

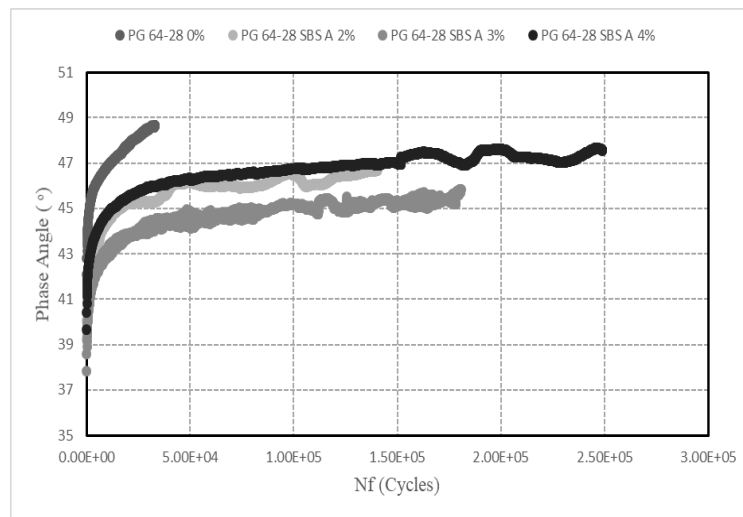


Figure 4-7 Phase Angle δ (°) Versus $Nf_{50\%}$ at 700 $\mu\text{m/m}$ PG 64-28

4.2 Hot Mix Failure Criteria and Fatigue Life Results

The results of the 4PB testing are shown by the number of cycles needed to reach 50% of the original value of the stiffness at 700 $\mu\text{m}/\text{m}$ as shown in Figure 4-8. Two samples were tested for each binder and an average of the two was taken. For both the PG 58-28 and PG 64-28 binders, the cycles go up with each polymer modification. The number of cycles to failure was 58,024 and 31,950 cycles on average, for the virgin binders for PG 58-28 and PG 64-28, respectively. The polymer modified binders had a minimum $N_{f50\%}$ of approximately 130,000 cycles and reached as high as 2.7 million cycles. We can see a major effect of polymer concentration in the binders on the fatigue life in the 4PB of the asphalt mixtures involved. This agrees with the findings in previous research [2], [37], [106].

The PG 58-28 showed higher fatigue with increased polymer (2-4% SBS), where it went from between 350,000 cycles to 2.7 million. The increase in cycles for PG 64-28 with higher polymer (2-4%), only went from 130,000 cycles to almost 200,000. The results show that the original binder properties have a major part to play in determining the fatigue life of the new PMAC mixtures. There is a strong possibility that the testing temperature of 20 °C played a role in favoring the PG 58-28, as the 64-28 may perform better at higher temperatures.

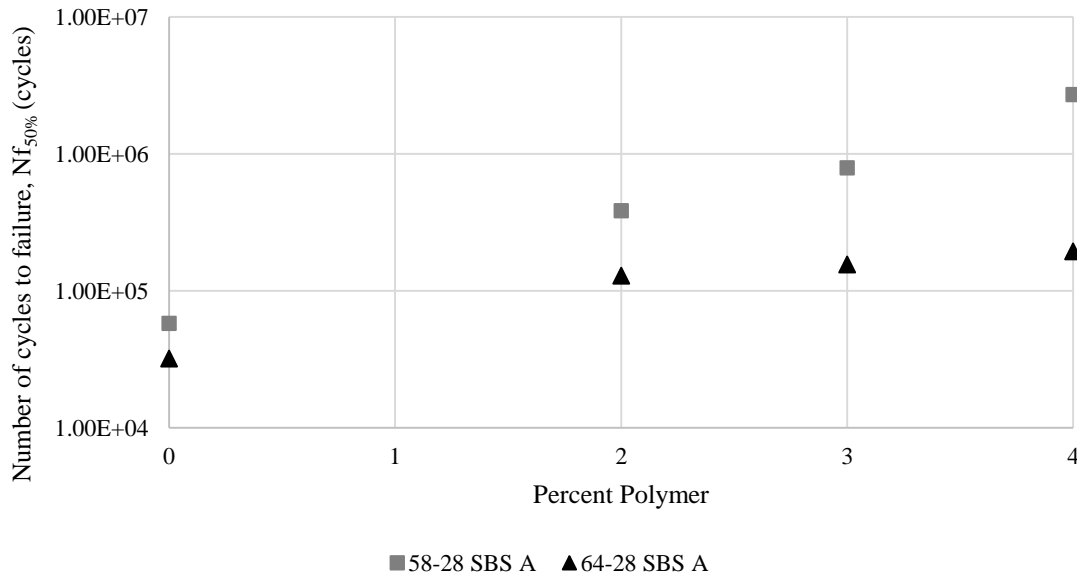


Figure 4-8 Comparison of Log $N_{f50\%}$ at 700 $\mu\text{m}/\text{m}$ versus percent polymer for PG 58-28 and PG 64-28

The samples were tested at different strain levels in the range of 300-1000 $\mu\text{m/m}$, to understand fatigue performance at different loading amplitudes, corresponding to different types of road traffic the asphalt would be subjected to in the field as depicted in Figures 4-9 and 4-10. Higher amplitudes mean lower fatigue life. Not every sample was tested at every strain level, as the samples that had longer fatigue life were then tested at higher amplitudes. The results confirm that increased polymer concentration means increased fatigue life, especially at the 400 and 500 $\mu\text{m/m}$ amplitudes. Comparing the fatigue life of the PG 64-28 and PG 58-28 at 700 $\mu\text{m/m}$ shows that the PG 64-28 has a lower fatigue life compared to PG 58-28 which indicates that PG 64-28 does not perform nearly as well at all levels. From another point of view, the softer binder PG 58-28 with the difference of the SBS polymer percentage, has a better fatigue life for PG 58-28 at the same strain level than the stiffer binder represented by PG 64-28.

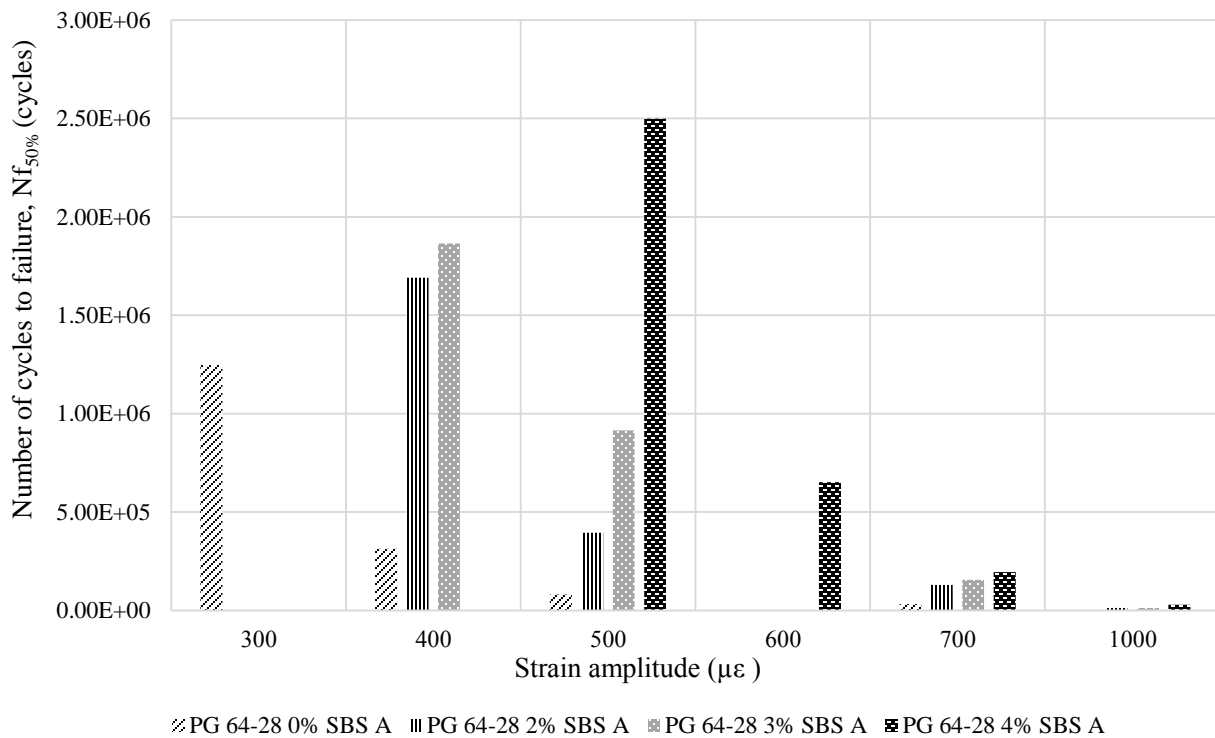


Figure 4-9 $N_{f50\%}$ versus strain level for PG 64-28

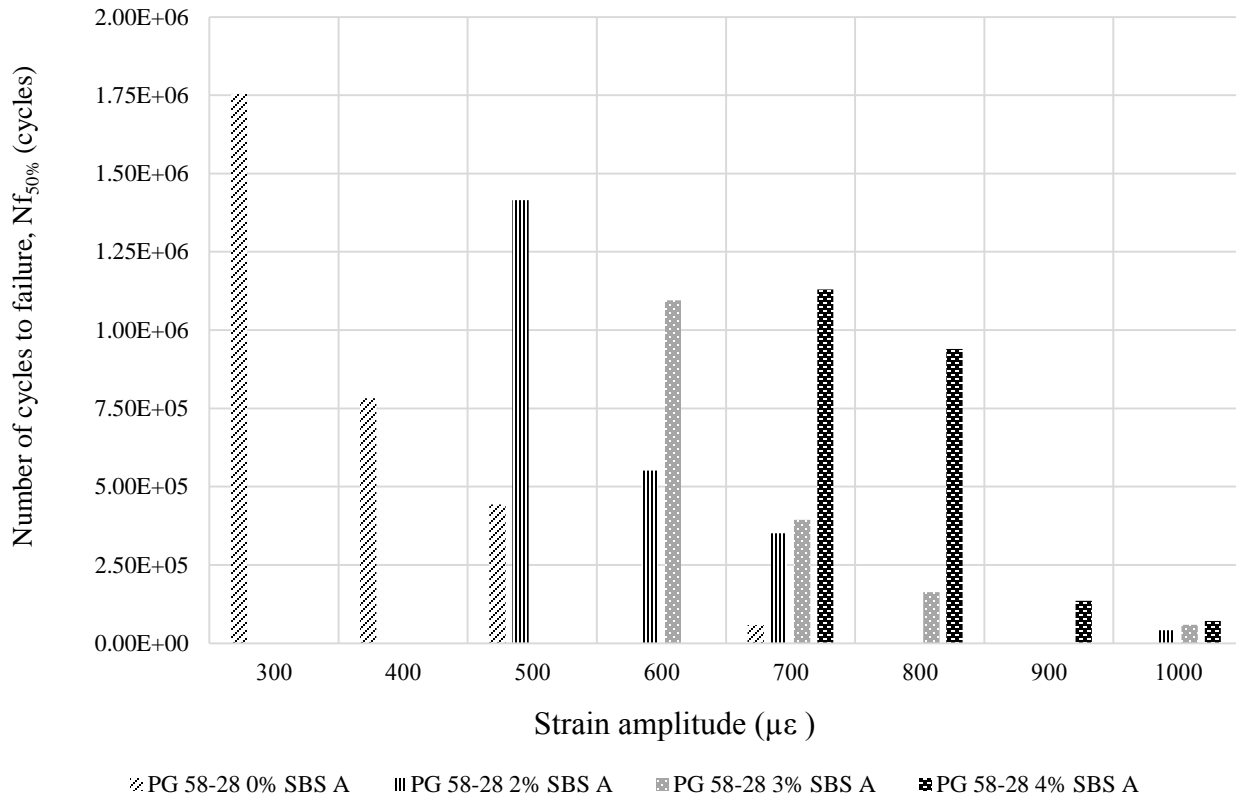


Figure 4-10 $N_{f50\%}$ versus strain level for PG 58-28

4.3 WÖHLER (or Fatigue) Curve and Determination of " ϵ_6 "

The WÖHLER (or fatigue) curves were obtained " ϵ_6 " for each mixture with SBS A. The results show a clear improvement when the polymer concentration was increased. Figure 4-11 shows the " ϵ_6 " for PG 64-28 with 0%, 2%, 3%, and 4%, respectively; the results indicate that with unmodified 0% " ϵ_6 " equals 280 $\mu\text{m/m}$ while the other mixes that containing SBS polymer had 408, 433, and 538 $\mu\text{m/m}$ respectively. It is the same trend with PG 58-28, the " ϵ_6 " for 0%, 2%, 3% and 4% are 301, 515, 635, and 768 $\mu\text{m/m}$, respectively as demonstrated in Figure 4-12. The linearity for both mixes was very good as shown by the R-values.

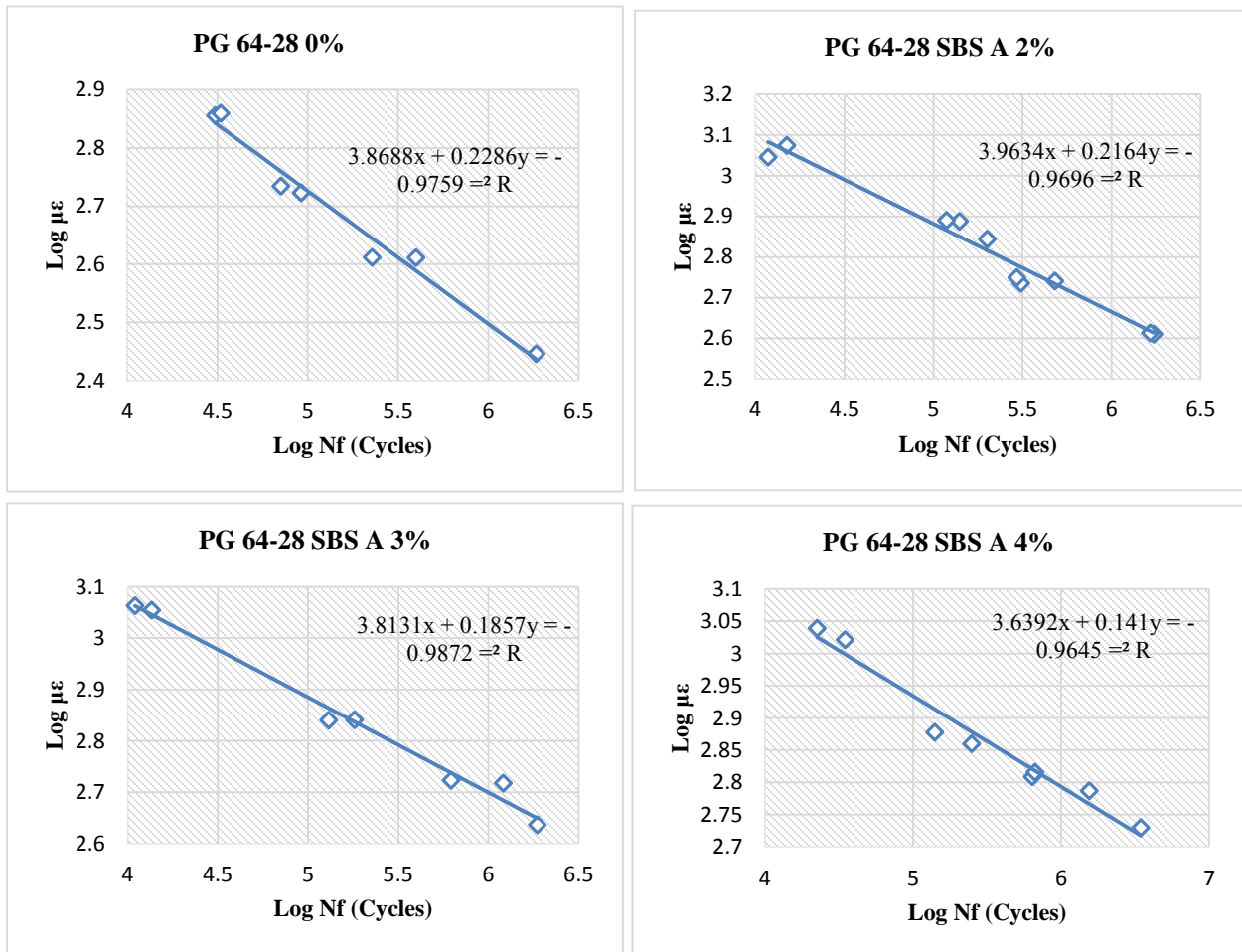


Figure 4-11 WÖHLER curve and obtaining "E₆" for PG 64-28

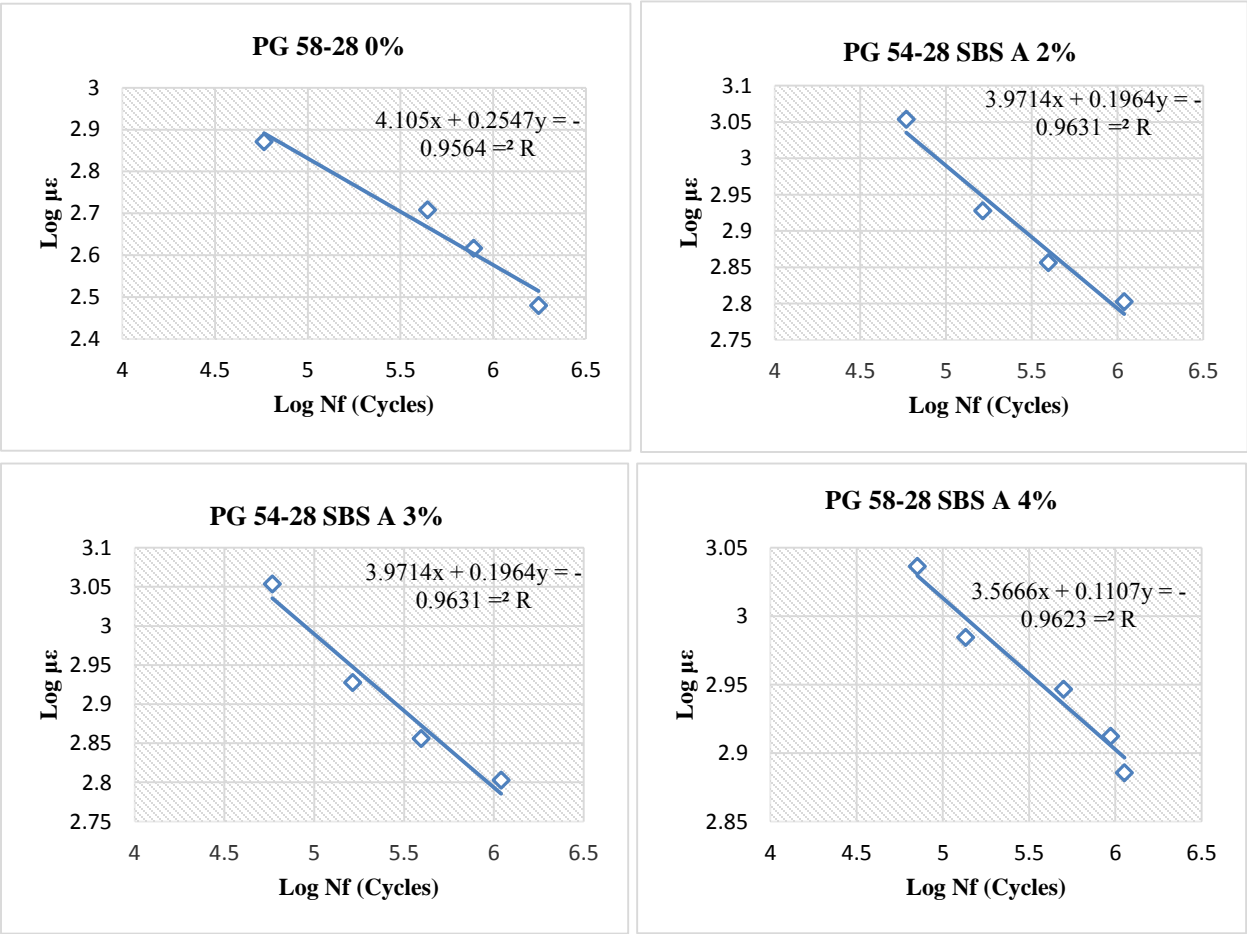


Figure 4-12 WÖHLER curve and obtaining "ε₆" for PG 58-28

It was noted that the " ϵ_6 " values for PG 58-28 are greater overall, compared to PG 64-28 as shown in Figure 4-13. This shows the importance of the base binder with polymer additives. This could be due to the higher stiffness of PG 64-28 but could also have to do with the specific binder chemistry in blending.

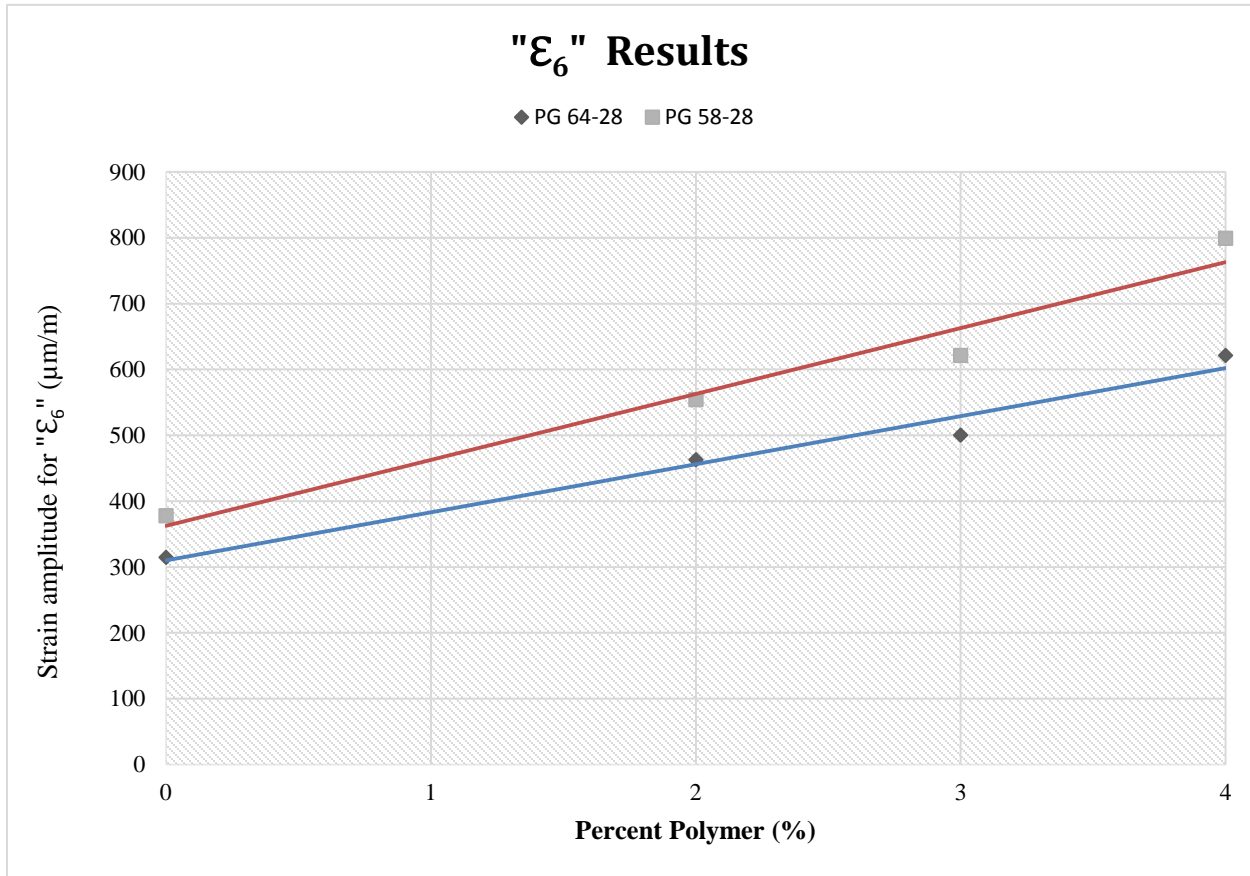


Figure 4-13 " ϵ_6 " values for PG 58-28 and PG 64-28

4.4 Damage Rate Analysis "DGCB"

The stiffness modulus data for each sample are used to determine the value a_{F1} , a_{F2} , a_{F3} and a_{F4} , fatigue slopes for intervals 1, 2, 3, and 4. Figure 4-14 illustrates the intervals for a sample. In addition, the values ϵ_{i1} , ϵ_{i2} , ϵ_{i3} , and ϵ_{i4} corresponding to the average strain level for each interval, were obtained. In Figures 4-15 to 4-22, the fatigue damage rate slopes for mixes are presented, versus the average strain for each interval.

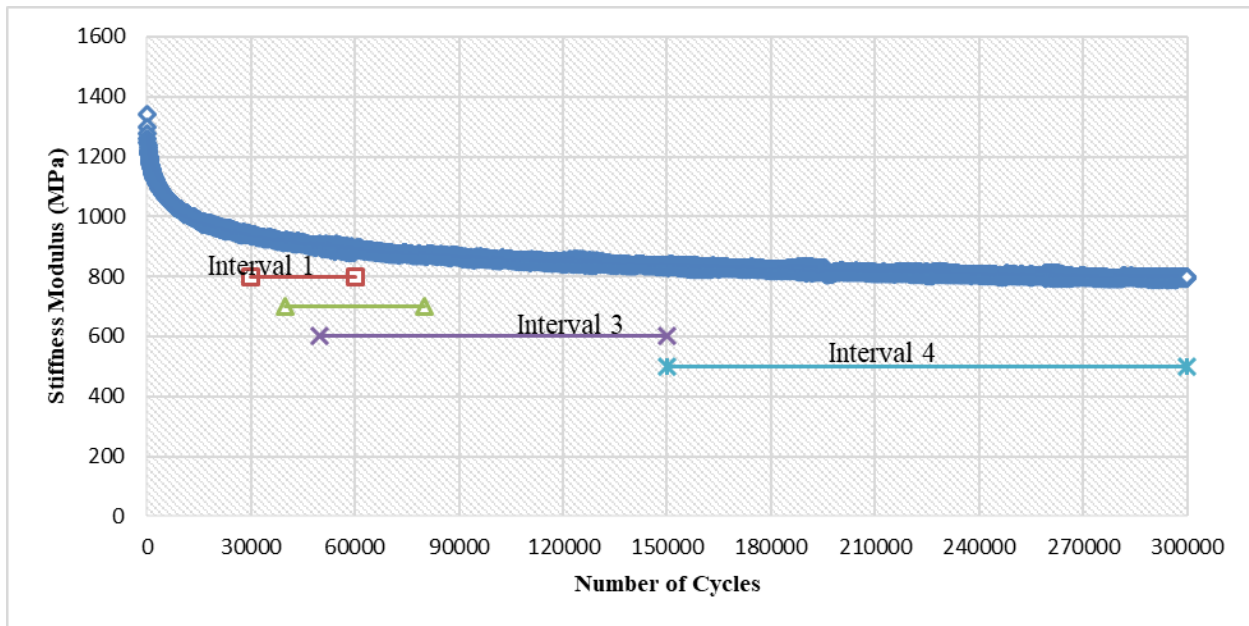


Figure 4-14 Application for different intervals PG 58-28 SBS A 4% at 700 $\mu\text{m/m}$

Figures 4-15 to 4-22 indicate that the damage rates are influenced by the rate of SBS modification. It can be clearly seen that the damage rate increases with higher strain levels and decreases with higher polymer concentration. Taking unmodified asphalt PG 58-28 in Figure 5-15 compared to modified asphalt PG 58-28 SBS A 2%, 3%, and 4%, respectively as an example, gives a picture of how the polymer influences the damage rates. By increasing the polymer content, the damage rate decreases substantially, up to values of 4%. This was also found in PMA mixes by ENTPE [14], [15]. This shows the ability of polymers to improve the damage resistance of asphalt mixtures undergoing various levels of fatigue loading. It was noted that the reduction in damage seems to be higher, when comparing the results at higher strain levels.

PG 64-28 binder exhibited a similar response in general to PG 58-28, except for some inconsistent values for fatigue slopes, especially in the case of PG 64-28 SBS A 3%. This may be due to an inconsistency in the binder properties or the non-homogeneity in the 4-point bending fatigue test [101].

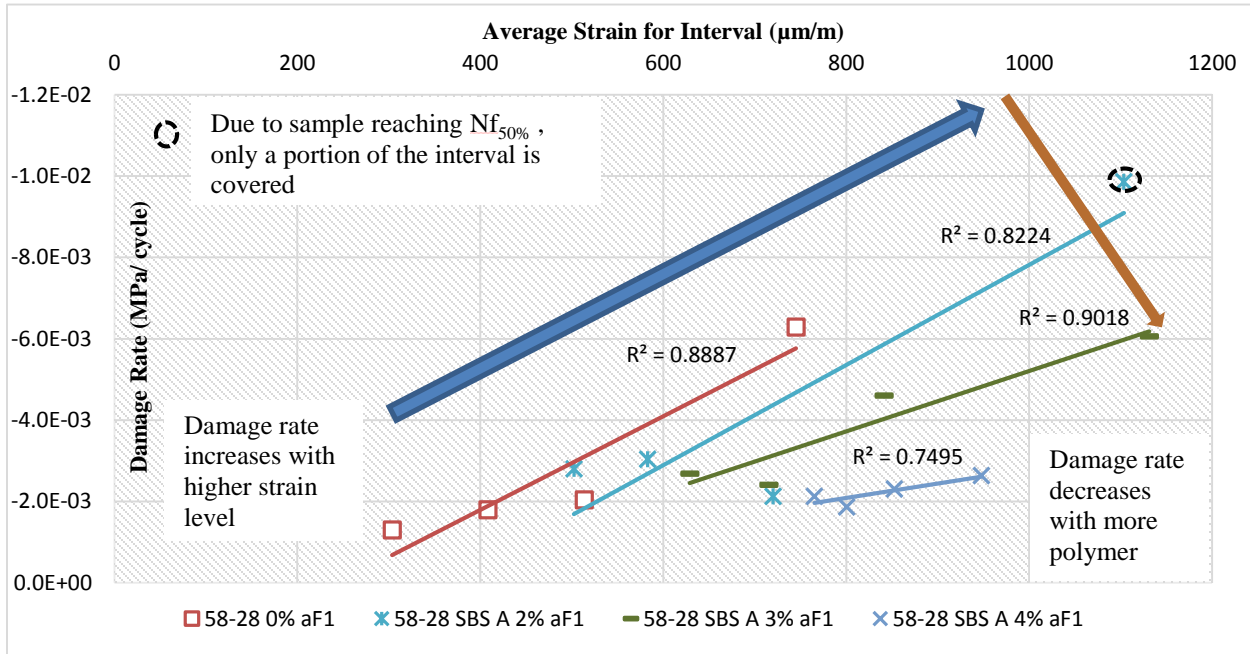


Figure 4-15 Damage rate PG 58-28 for interval II = (30000 to 60000 cycles)

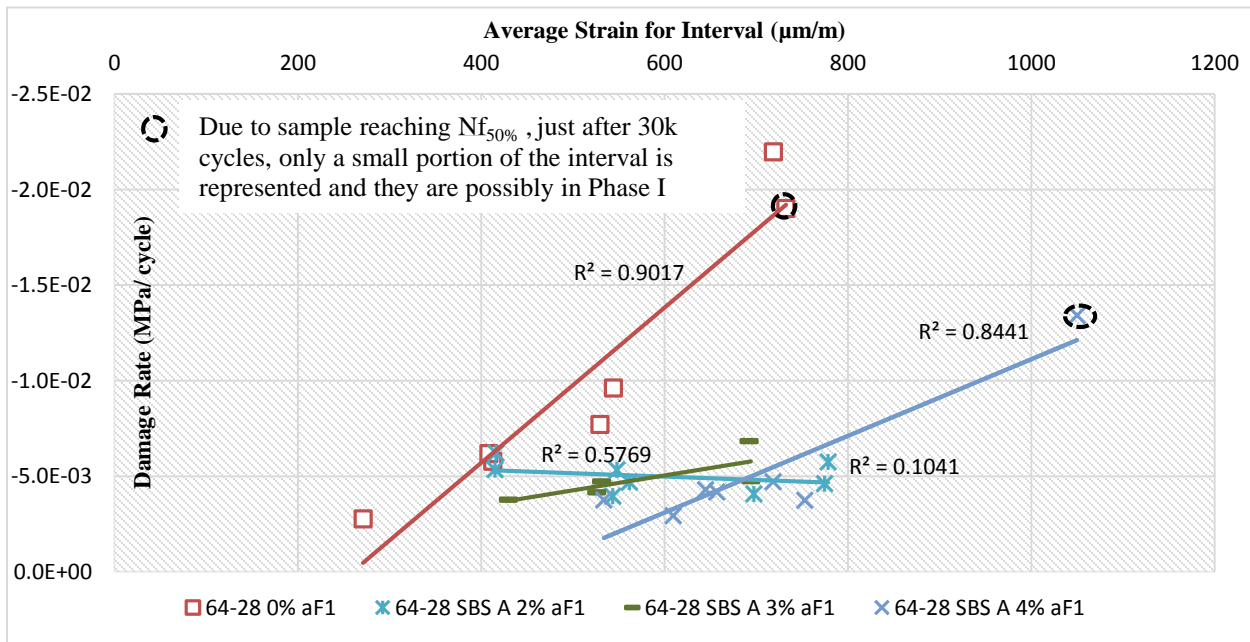


Figure 4-16 Damage rate PG 64-28 for interval II = (30000 to 60000 cycles)

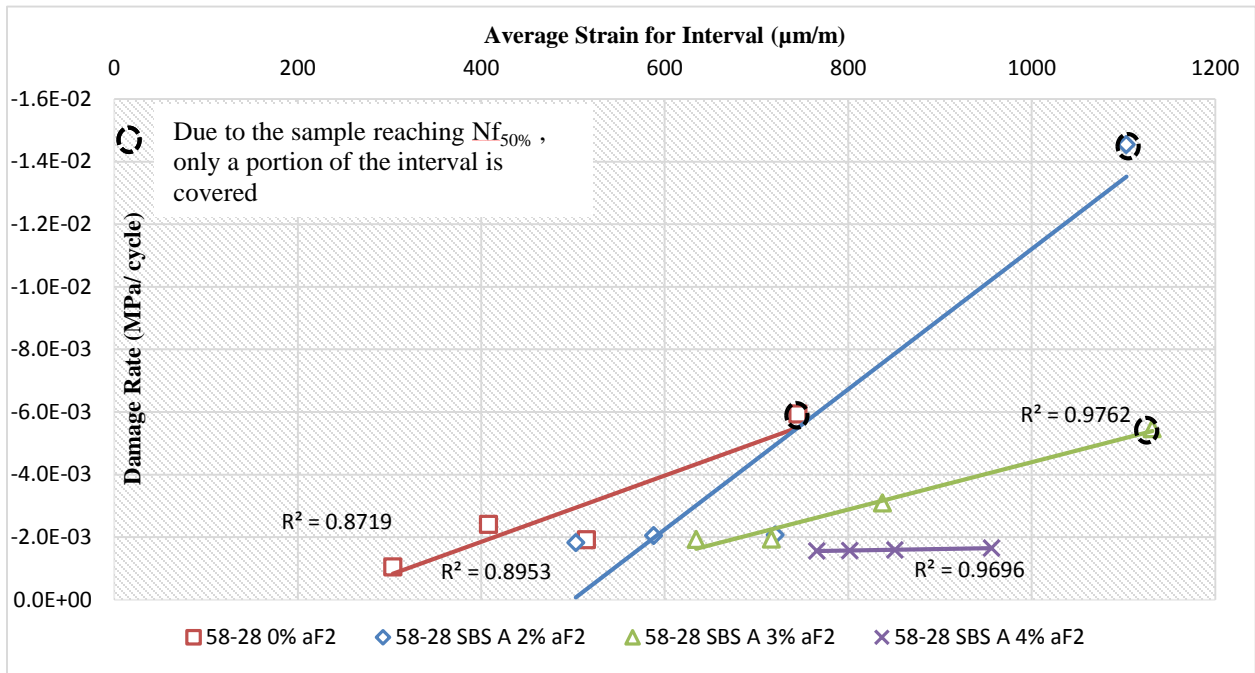


Figure 4-17 Damage rate PG 58-28 for interval I2 = (40000 to 80000 cycles)

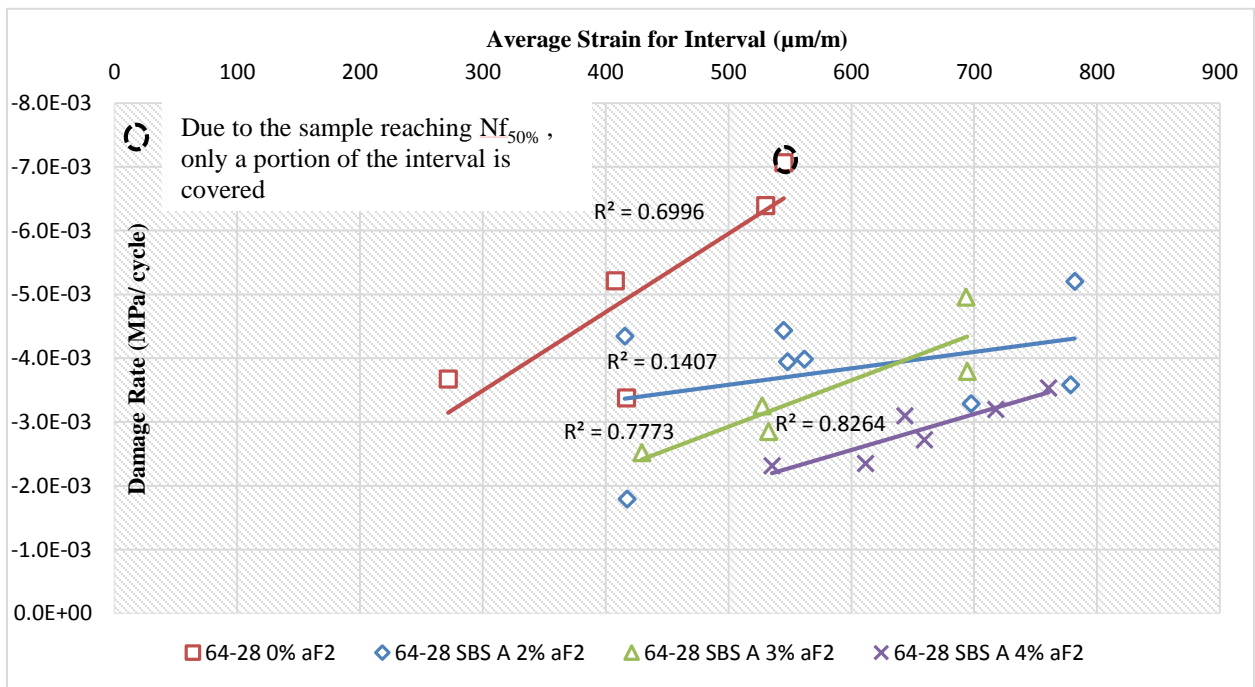


Figure 4-18 Damage rate PG 64-28 for interval I2 = (40000 to 80000 cycles)

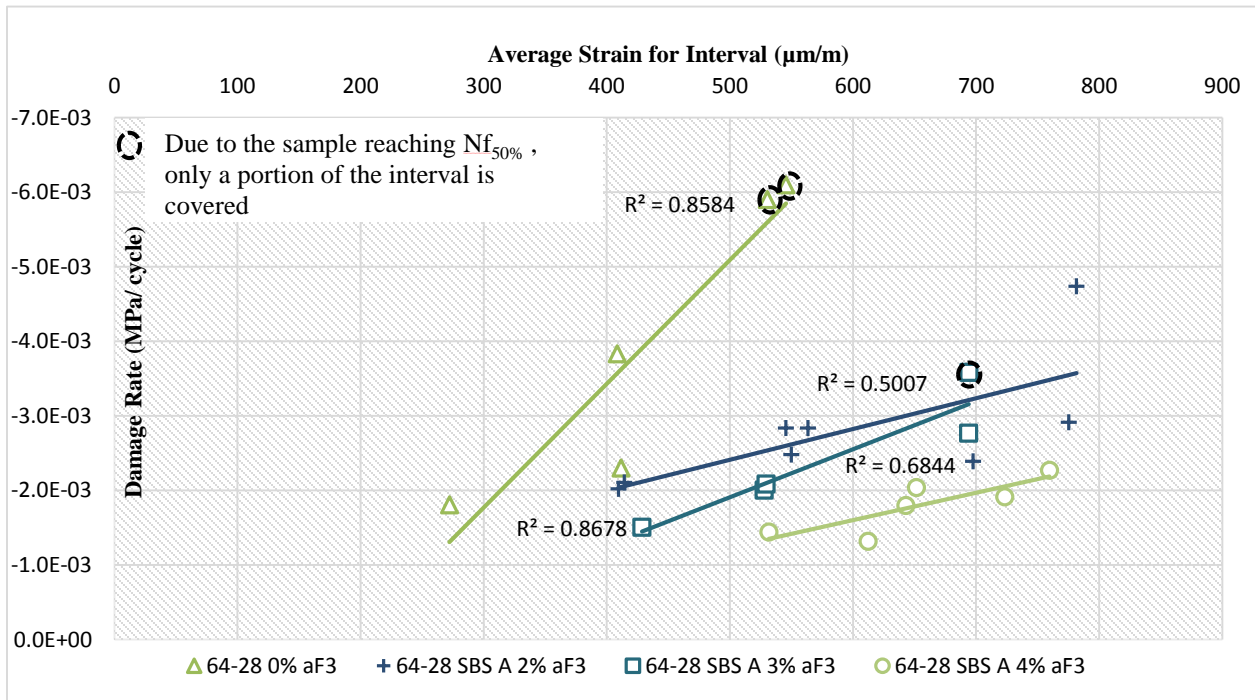


Figure 4-19 Damage rate PG 58-28 for interval I3= (50000 to 150000 cycles)

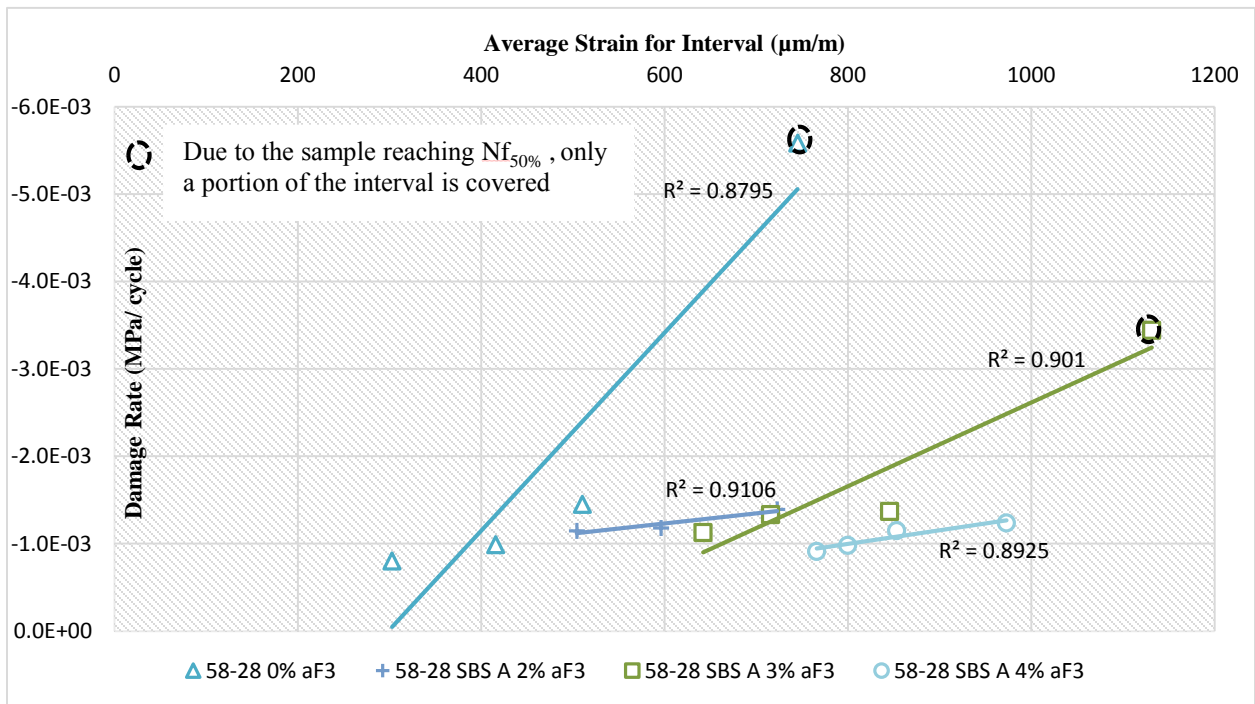


Figure 4-20 Damage rate PG 64-28 for interval I3= (50000 to 150000 cycles)

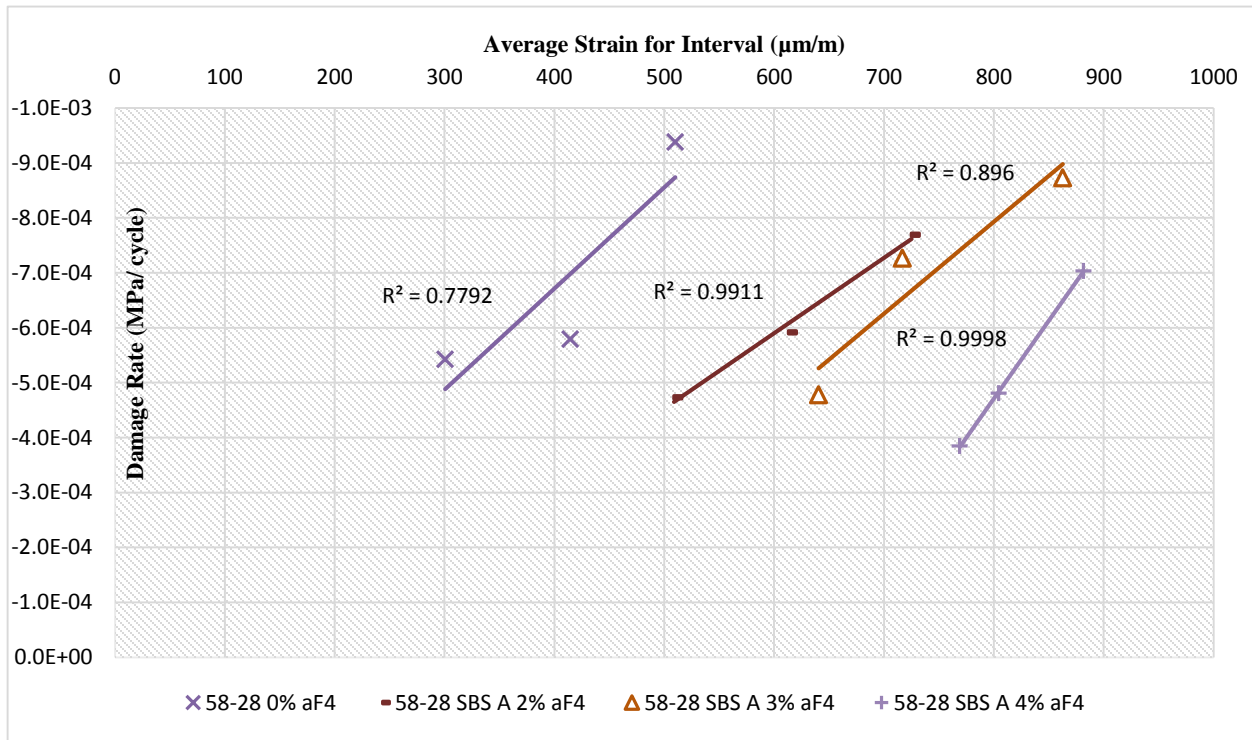


Figure 4-21 Damage rate PG 58-28 for interval I4 = (150000 to 300000 cycles)

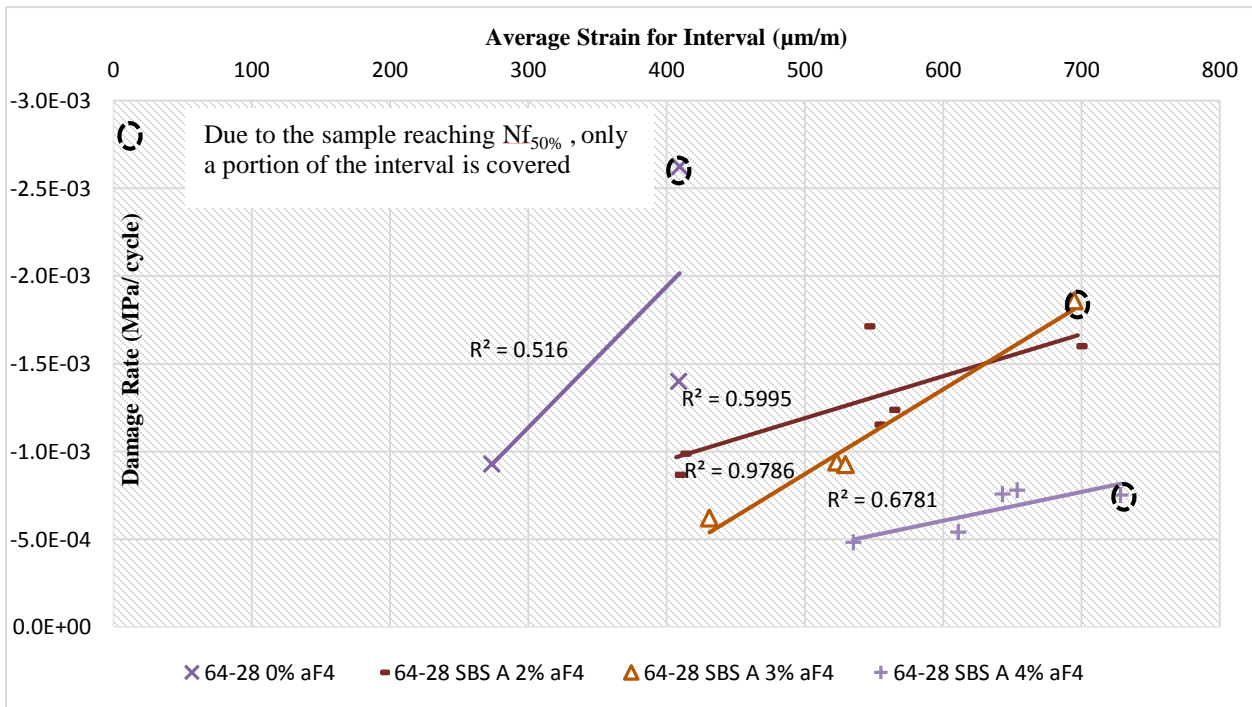


Figure 4-22 Damage rate PG 64-28 for interval I4 = (150000 to 300000 cycles)

Table 4-3 and 4-4 present the linearity of both binders with a different polymer rate. For PG 58-28, in general, the linearity is acceptable, however with PG 64-28 the results are not as good as for PG 58-28. There are some measurements that may need to be retested.

Table 4-3 R-Values for PG 58-28

PG 58-28	0%SBS	2%SBS	3%SBS	4%SBS
R ² 1	0.889	0.822	0.902	0.749
R ² 2	0.872	0.895	0.976	0.970
R ² 3	0.880	0.911	0.901	0.893
R ² 4	0.779	0.991	0.896	1.000

Table 4-4 R-Values for PG 64-28

PG 64-28	0% SBS	2% SBS	3% SBS	4% SBS
R ² 1	0.902	0.104	0.577	0.844
R ² 2	0.700	0.141	0.777	0.826
R ² 3	0.858	0.501	0.868	0.684
R ² 4	0.516	0.600	0.979	0.678

Chapter 5 CONCLUSIONS, RECOMMENDATIONS AND FUTURE RESEARCH

5.1 Conclusions and Recommendations

Extensive investigations show that the fatigue life will be improved by adding SBS polymer into the asphalt mixtures. However, due to the complex compositions of asphalt cement, which contain different components and substances, each having different chemical and physical properties, these complex compositions must be covered in future works. In this project, the fatigue characterization of asphalt mixes with different percentages of SBS polymer modified asphalt cement were tested using 4PB. The mixes were evaluated using WÖHLER Curve and the “DGCB” methods, and the results can be summarized as follows:

- The fatigue life $N_{f50\%}$ of the asphalt mixtures increased with polymer addition for both binders and at all strain levels. At multiple strain levels, PG 64-28 shows lower fatigue life when compared to PG 58-28 at the same strain level. This may be due to the fact that the PG 64-28 is stiffer and may be more susceptible to cracking at this higher strain.
- Both fatigue analysis methods, by WÖHLER Curve and the “DGCB” Method, have shown that the addition SBS polymer improves the fatigue life and reduced the damage induced by fatigue. The SBS polymer addition resulted in a lower damage rate with PG 58-28 than with the PG 64-28, likely because of better compatibility between the SBS polymer and PG 58-28.
- Some inconsistencies in the damage results, especially for 64-28 at 3%, could be explained by the fact that the 4-point bending fatigue test is a non-homogenous test. However, these inconsistencies may also be due to the characteristics of the composition of the asphalt cement which were used in this project. Overall, it can be said that the 4PB may not be ideal for damage rate analysis.
- To have a comprehensive understanding of the fatigue behaviour in 4-point bending test, the test should go beyond the classical failure criterion $N_{f50\%}$ and should take into account

sample geometry, as it seemed to have an effect on the failure criteria. The tolerance range ($\pm 6\text{mm}$) in AASHTO T 312 for the 4PB test sample dimensions must be reconsidered, in particular for the beam thickness, as the variation of the sample dimensions can have a significant effect on fatigue characterization. Other test approaches should be used to present a more complete picture of fatigue performance, especially in terms of the homogeneous tension-compression test.

5.2 Future Research

Due to the limitations associated with the 4PB, additional fatigue testing needs to be performed to improve the fatigue characterization of the hot mix asphalt. Homogenous uniaxial tension-compression testing should be conducted on mixtures in order to better understand the role of polymer and binder on fatigue performance. A comprehensive approach needs to be developed in order to investigate the fatigue characterization of asphalt mixes with polymer modified asphalt cement by including all the biased effects.

Furthermore, a thorough investigation of the polymer modification additives to find the optimum percentage of polymer to be used can provide a significant improvement to the pavement's ability to resist general pavement distresses.

In terms of economics, more cost-effective asphalt modification needs to be considered. In addition, more research should be conducted to provide a better understanding of how polymer modified asphalt can be effectively used for short and long terms needs. More research that focuses on the maintenance and recycling of PMAC should be conducted in the future. Finally, environmental concerns need to be looked at as well.

References

- [1] D. Perraton, H. Baaj, and A. Carter, “Comparison of Some Pavement Design Methods from a Fatigue Point of View: Effect of Fatigue Properties of Asphalt Materials,” *Road Mater. Pavement Des.*, vol. 11, no. 4, pp. 833–861, 2010.
- [2] H. Baaj, D. Perraton, H. Di Benedetto, and M. Paradis, “Contribution à l’étude de la relation entre le module complexe et la résistance à la fatigue et à l’orniérage pour l’enrobé SMA,” in *Proceedings of the Forty-Eighth Annual Conference of the Canadian Technical Asphalt Association (CTAA)*: Halifax, Nova Scotia, 2003.
- [3] H. Baaj, P. Mikhailenko, H. Almutairi, and H. Di Benedetto, “Recovery of asphalt mixture stiffness during fatigue loading rest periods,” *Constr. Build. Mater.*, vol. 158, pp. 591–600, 2018.
- [4] TAC, “TAC Primer: Pavement Asset Design and Management Guide,” no. March, pp. 1–13, 2014.
- [5] FHWA, “HMA Pavement Mix Type Selection Guide,” pp. 1–24, 2001.
- [6] A Copeland, “Reclaimed Asphalt Pavement in Asphalt Mixtures: State of the Practice,” Rep. No. FHWA-HRT-11-021, no. FHWA, p. McLean, Virginia, 2011.
- [7] W. R. Kingery, “Laboratory study of fatigue characteristics of HMA surface mixtures containing recycled asphalt pavement (RAP),” 2004.
- [8] S. T. AASHTO, “Standard method of test for determining the fatigue life of compacted hot-mix asphalt (HMA) subjected to repeated flexural bending,” T321-03, 2007.
- [9] N. Tapsoba, C. Sauzéat, H. Di Benedetto, H. Baaj, and M. Ech, “Three-dimensional analysis of fatigue tests on bituminous mixtures,” *Fatigue Fract. Eng. Mater. Struct.*, vol. 38, no. 6, pp. 730–741, 2015.
- [10] J. J. Emery, “Evaluation and Mitigation of Asphalt Pavement Top-Down Cracking,” *Annu. Conf. Transp. Assoc. Canada*, 2006.
- [11] F. Zhou, S. Hu, and T. Scullion, “Integrated Asphalt (Overlay) Mixture Design, Balancing Rutting and Cracking Requirements,” *FHWA Rep.*, vol. 7, no. 2, p. 162, 2006.
- [12] H. Di Benedetto, C. de La Roche, H. Baaj, A. Pronk, and R. Lundström, “Fatigue of bituminous mixtures,” *Mater. Struct.*, vol. 37, no. 3, pp. 202–216, 2004.
- [13] G. M. Rowe and M. G. Bouldin, “Improved techniques to evaluate the fatigue resistance of asphaltic mixtures,” in *2nd Eurasphalt & Eurobitume Congress Barcelona*, 2000, vol. 2000.

- [14] H. Baaj, H. Di Benedetto, and P. Chaverot, "Fatigue of mixes: an intrinsic damage approach," in *Sixth International RILEM Symposium on Performance Testing and Evaluation of Bituminous Materials*, 2003, pp. 394–400.
- [15] H. Baaj, H. Di Benedetto, and P. Chaverot, "Effect of binder characteristics on fatigue of asphalt pavement using an intrinsic damage approach," *Road Mater. Pavement Des.*, vol. 6, no. 2, pp. 147–174, 2005.
- [16] H. Baaj, M. Ech, P. Lum, and R. W. Forfyflow, "Behaviour of Asphalt Mixes Modified with High Rates of Asphalt Shingle Modifier (ASM) and Reclaimed Asphalt Pavement (RAP)," in *The Fifty-sixth Annual Conference of the Canadian Technical Asphalt Association* Canadian Technical Asphalt Association, 2011.
- [17] Y. H. Huang, "Pavement analysis and design," 1993.
- [18] H. Di Benedetto, "Modélisation: écart entre état des connaissances et applications," *Journée LAVOC, École Polytech. fédérale Lausanne, Lausanne, Suisse*, 1998.
- [19] S. Mangiafico, "Linear viscoelastic properties and fatigue of bituminous mixtures produced with reclaimed asphalt pavement and corresponding binder blends," *ENTPE, Lyon*, 2014.
- [20] U. Viscoelastic and C. Damage, "Project No . NCHRP 9-44 A Validating an Endurance Limit for HMA Pavements: Laboratory Experiment and Algorithm Development Endurance Limit for HMA Based on Healing Phenomena Using Viscoelastic Continuum Damage Analysis," no. July, 2013.
- [21] R. B. McGennis, R. M. Anderson, T. W. Kennedy, and M. Solaimanian, "Background of superpave asphalt mixture design and analysis. National asphalt training center demonstration project 101. Final report, December 1992-November 1994," *Asphalt Inst., Lexington, KY (United States)*, 1995.
- [22] H. Di Benedetto, B. Delaporte, and C. Sauzéat, "Three-dimensional linear behavior of bituminous materials: experiments and modeling," *Int. J. Geomech.*, vol. 7, no. 2, pp. 149–157, 2007.
- [23] F. Olard, H. Di Benedetto, A. Dony, and J.-C. Vaniscote, "Properties of bituminous mixtures at low temperatures and relations with binder characteristics," *Mater. Struct.*, vol. 38, no. 1, pp. 121–126, 2005.
- [24] H. Di Benedetto, M. N. Partl, L. Francken, and C. De La Roche, "Stiffness testing for bituminous mixtures. RILEM TC 182-PEB Performance Testing and Evaluation of Bituminous Materials," *Mater. Struct.*, vol. 34, no. March, pp. 66–70, 2001.
- [25] M. Abojaradeh, "Predictive fatigue models for Arizona asphalt concrete mixtures." *Arizona State University*, 2003.

- [26] F. L. Roberts, P. S. Kandhal, E. R. Brown, D.-Y. Lee, and T. W. Kennedy, "Hot mix asphalt materials, mixture design and construction," 1991.
- [27] D. N. Little, R. L. Lytton, D. Williams, and C. W. Chen, "Microdamage healing in asphalt and asphalt concrete, Volume 1: microdamage and microdamage healing, project summary report," Turner-Fairbank Highway Research Center, 2001.
- [28] H. Baaj, "Comportement à la fatigue des matériaux granulaires traités aux liants hydrocarbonés [Fatigue behaviour of granular materials treated with hydrocarbon binders]," p. 267, 2002.
- [29] A. Institute., *The Asphalt handbook*. Lexington, Ky.: Asphalt Institute, 2007.
- [30] S. A. Romanoschi, N. I. Dumitru, O. Dumitru, and G. Flager, "Dynamic Resilient Modulus and the Fatigue Properties of Superpave HMA Mixes Used in the Base Layer of Kansas Flexible Pavements," in 85th Annual Meeting of the Transportation Research Board, Washington, DC, 2006.
- [31] H. Wen, "Fatigue performance evaluation of WesTrack asphalt mixtures based on viscoelastic analysis of indirect tensile test," 2001.
- [32] S. Abo-Qudais and I. Shatnawi, "Prediction of bituminous mixture fatigue life based on accumulated strain," *Constr. Build. Mater.*, vol. 21, no. 6, pp. 1370–1376, 2007.
- [33] F. M. Nejad, E. Aflaki, and M. A. Mohammadi, "Fatigue behavior of SMA and HMA mixtures," *Constr. Build. Mater.*, vol. 24, no. 7, pp. 1158–1165, 2010.
- [34] P. Baburamani, *Asphalt fatigue life prediction models: a literature review*, no. ARR 334. 1999.
- [35] I. Hafeez, M. A. Kamal, M. W. Mirza, and S. Bilal, "Laboratory fatigue performance evaluation of different field laid asphalt mixtures," *Constr. Build. Mater.*, vol. 44, pp. 792–797, 2013.
- [36] K. Mollenhauer, M. Wistuba, and R. Rabe, "Loading frequency and fatigue: In situ conditions & impact on test results," in 2nd Workshop on Four Point Bending, 2009, pp. 24–25.
- [37] M. Fakhri, K. Hassani, and A. R. Ghanizadeh, "Impact of loading frequency on the fatigue behavior of SBS modified asphalt mixtures," *Procedia-Social Behav. Sci.*, vol. 104, pp. 69–78, 2013.
- [38] S. Adhikari and Z. You, "Fatigue evaluation of asphalt pavement using beam fatigue apparatus," *Technol. Interface J.*, vol. 10, no. 3, 2010.

- [39] W. Van Dijk, "Practical fatigue characterization of bituminous mixes," *J. Assoc. Asph. Paving Technol.*, vol. 44, pp. 38–72, 1975.
- [40] D. N. Little, J. W. Button, Y. Kim, J. Ahmmed, and T. T. Institt, "Mechanistic evaluation of selected asphalt additives," 1987.
- [41] A. A. Tayebali, J. A. Deacon, J. S. Coplan, J. T. Harvey, and C. L. Monismith, "Mix and mode-of-loading effects on fatigue response of asphalt-aggregate mixes," *J. Assoc. Asph. Paving Technol.*, vol. 63, pp. 118–151, 1994.
- [42] C. L. Monismith, "Non-traffic Load Associated Cracking of Asphalt Pavements: Symposium," 1966.
- [43] W. A. J. Albert, "Über Treibseile am Harz. *Archiv für Mineralogie, Geognosie*," *Bergbau und Huttenkd.*, vol. 10, p. 215, 1837.
- [44] J. V. Poncelet, *Introduction à la mécanique industrielle, physique ou expérimentale*. Thiel, 1839.
- [45] A. Wöhler, *Über die Festigkeits-versuche mit Eisen und Stahl*. 1870.
- [46] P. S. Pell and K. E. Cooper, "The effect of testing and mix variables on the fatigue performance of bituminous materials," *J. Assoc. Asph. Paving Technol.*, vol. 44, pp. 1–37, 1975.
- [47] A. A. Tayebali, G. M. Rowe, and J. B. Sousa, "Fatigue response of asphalt-aggregate mixtures (with discussion)," *J. Assoc. Asph. Paving Technol.*, vol. 61, 1992.
- [48] G. M. Rowe, "Performance of asphalt mixtures in the trapezoidal fatigue test," *Asph. Paving Technol.*, vol. 62, p. 344, 1993.
- [49] A. C. Pronk and P. C. Hopman, "Energy Dissipation: The Leading Factor of Fatigue," *Proc. the Conference United States Strateg. Highw. Program*. London Elsevier Sci. Publ. 2ss —, vol. 267, 1990.
- [50] Y. R. Kim, H.-J. Lee, and D. N. Little, "Fatigue characterization of asphalt concrete using viscoelasticity and continuum damage theory (with discussion)," *J. Assoc. Asph. Paving Technol.*, vol. 66, 1997.
- [51] R. Reese, "Properties of aged asphalt binder related to asphalt concrete fatigue life," *J. Assoc. Asph. Paving Technol.*, vol. 66, 1997.
- [52] J. S. Daniel, *Development of a simplified fatigue test and analysis procedure using a viscoelastic, continuum damage model and its implementation to WesTrack mixtures*. 2001.

- [53] A. Tayebali, J. Deacon, J. Coplantz, J. Harvey, and C. Monismith, "Fatigue response of asphalt aggregate mixtures. Part I-Test method selection, Strategic Highway Research Program, Project A-404, Asphalt Research Program, Institute of Transportation Studies," Univ. California-Berkeley, 1994.
- [54] M. A. Ashayer Soltani, "Comportement en fatigue des enrobés bitumeux." Lyon, INSA, 1998.
- [55] H. Di Benedetto, A. Ashayer Soltani, and P. Chaverot, "Fatigue damage for bituminous mixtures: a pertinent approach," *J. Assoc. Asph. Paving Technol.*, vol. 65, 1996.
- [56] H. Di Benedetto, A. Ashayer Soltani, and P. Chaverot, "Fatigue damage for bituminous mixtures," in *Proceedings of The Fifth International Rilem Symposium MTBM Lyon*, 1997.
- [57] H. Di Benedetto, C. de La Roche, H. Baaj, A. Pronk, and R. Lundstrom, "Fatigue of bituminous mixtures: different approaches and RILEM group contribution," in *Sixth International RILEM Symposium on Performance Testing and Evaluation of Bituminous Materials*, 2003, pp. 15–38.
- [58] H. Baaj, H. Di Benedetto, and P. Chaverot, "Different experimental approaches and criteria for fatigue of asphalt mixes," in *Proceedings of the Forty-Ninth Annual Conference of the Canadian Technical Asphalt Association (CTAA)-Montreal, Quebec*, 2004.
- [59] R. Roque, B. Birgisson, C. Drakos, and G. Sholar, "GUIDELINES FOR USE OF MODIFIED BINDERS," University of Florida, Final Report UF Project No. 4910-4504-964-12, Mar. 2005.
- [60] C. de La Roche, J. F. Corte, J. C. Gramsammer, H. Odéon, L. Tiret, and G. Caroff, "Étude de la fatigue des enrobés bitumineux à l'aide du manège de fatigue du LCPC," *Rev. Gen. des Routes des Aerodromes*, no. 716, pp. 62–75, 1994.
- [61] H. R. B., *The AASHO Road Test: History and Description of Project*. National Academy of Sciences, 1961.
- [62] Aurilio M., Qabur A., Mikhailenko P. Baaj H., Comparing the Fatigue Performance of HMA Samples with PMA to their Multiple Stress Creep Recovery and Double Notched Tension Test Properties, submitted for publication at the Annual Conference of Canadian Technical Asphalt Association, Regina, November 2018
- [63] F. Zhou et al., "Experimental design for field validation of laboratory tests to assess cracking resistance of asphalt mixtures." Texas Transportation Institute Texas A&M University Project, 2016.
- [64] Y. Becker, M. P. Méndez, and Y. Rodríguez, "Polymer modified asphalt," *Vis. Tecnol.*, vol. 9, no. 1, pp. 39–50, 2001.

- [65] O. Yetkin, I. Tek, F. Yetkin, and N. Numanoglu, "Role of pleural viscosity in the differential diagnosis of exudative pleural effusion," *Respirology*, vol. 12, no. 2, pp. 267–271, 2007.
- [66] A. W. Monks, H. M. White, and D. C. Bassett, "On shish-kebab morphologies in crystalline polymers," *Polymer (Guildf.)*, vol. 37, no. 26, pp. 5933–5936, 1996.
- [67] K. J. Button and D. Swann, "Preface," *Antitrust Bull.*, vol. 37, no. 2, p. 281, Jun. 1992.
- [68] T. Alataş and M. Yilmaz, "Effects of different polymers on mechanical properties of bituminous binders and hot mixtures," *Constr. Build. Mater.*, vol. 42, pp. 161–167, May 2013.
- [69] C. Gorkem and B. Sengoz, "Predicting stripping and moisture induced damage of asphalt concrete prepared with polymer modified bitumen and hydrated lime," *Constr. Build. Mater.*, vol. 23, no. 6, pp. 2227–2236, Jun. 2009.
- [70] S. Tayfur, H. Ozen, and A. Aksoy, "Investigation of rutting performance of asphalt mixtures containing polymer modifiers," *Constr. Build. Mater.*, vol. 21, no. 2, pp. 328–337, Feb. 2007.
- [71] J. Ponniah and G. Kennepohl, "Crack Sealing in Flexible Pavements: A Life-Cycle Cost Analysis," *Transp. Res. Rec. J. Transp. Res. Board*, vol. 1529, pp. 86–94, 1996.
- [72] U. Isacson and X. Lu, "Testing and appraisal of polymer modified road bitumens-state of the art," *Mater. Struct.*, vol. 28, no. 3, pp. 139–159, 1995.
- [73] J. Newman, *Polymer-modified asphalt mixtures for heavy-duty pavements: fatigue characteristics as measured by flexural beam* 2018.
- [74] L. H. Lewandowski, "Polymer Modification of Paving Asphalt Binders," *Rubber Chem. Technol.*, vol. 67, no. 3, pp. 447–480, Jul. 1994.
- [75] V. Mouillet, F. Farcas, and E. Chailleux, "Physico-chemical techniques for analysing the ageing of polymer modified bitumen," in *Polymer Modified Bitumen*, Elsevier, 2011, pp. 366–395.
- [76] P. Mikhailenko, H. Kadhim, H. Baaj, and S. Tighe, "Observation of asphalt binder microstructure with ESEM," *J. Microsc.*, vol. 267, no. 3, pp. 347–355, 2017.
- [77] Y. Yildirim, "Polymer modified asphalt binders," *Constr. Build. Mater.*, vol. 21, no. 1, pp. 66–72, 2007.
- [78] M. M. J. Jacobs and B. W. Sluer, "Fatigue testing of polymer modified asphalt mixtures," in *2nd Workshop on Four Point Bending*, 2009.
- [79] A. J. Hoiberg, "Bituminous materials: asphalts, tars and pitches volume iii coal tars and

- pitches,” 1966.
- [80] G. D. AIREY, “Rheological Characteristics of Polymer Modified and Aged Bitumens,” p. 256, 1997.
- [81] U. Isacson and X. Lu, “Testing and appraisal of polymer modified road bitumens—state of the art,” *Mater. Struct.*, vol. 28, no. 3, pp. 139–159, 1995.
- [82] P. B. Bamforth, K. N. Gurusamy, W. F. Price, J. L. Price, and W. J. McCarter, “Non-destructive testing on new and in-place concrete. the united states strategic highway research program. sharing the benefits. conference organized by the institution of civil engineers in cooperation with us strategic highway research program, 29th-31,” *Publ. Elsevier Appl. Sci. Publ. Ltd.*, 1990.
- [83] Y. Yildirim, A. Qatan, and J. A. Prozzi, “Field Performance Comparison of Hot Pour Sealants and Cold Pour Sealants,” in *Proceedings of the 8th Conference on Asphalt Pavements for Southern Africa (CAPSA’04)*, 2004, vol. 12, p. 16.
- [84] B. Sengoz and G. Isikyakar, “Analysis of styrene-butadiene-styrene polymer modified bitumen using fluorescent microscopy and conventional test methods,” *J. Hazard. Mater.*, vol. 150, no. 2, pp. 424–432, 2008.
- [85] C. Oliviero Rossi, A. Spadafora, B. Teltayev, G. Izmailova, Y. Amerbayev, and V. Bortolotti, “Polymer modified bitumen: Rheological properties and structural characterization,” *Colloids Surfaces A Physicochem. Eng. Asp.*, vol. 480, no. March, pp. 390–397, 2015.
- [86] Q. Li, F. Ni, L. Gao, Q. Yuan, and Y. Xiao, “Evaluating the rutting resistance of asphalt mixtures using an advanced repeated load permanent deformation test under field conditions,” *Constr. Build. Mater.*, vol. 61, pp. 241–251, 2014.
- [87] S. Wu, J. Han, and H. Wang, “Research on fatigue resistance performance of nano-rubber powder modified Asphalt,” *International Journal of Pavement Research and Technology*, vol. 2, no. 5. pp. 227–230, 2009.
- [88] J. H. Denning and J. Carswell, “Improvements in rolled asphalt surfacings by the addition of organic polymers,” 1981.
- [89] J. Read and D. Whiteoak, *The shell bitumen handbook*. Thomas Telford, 2003.
- [90] R. Shanks, “Thermoplastic starch,” in *Thermoplastic elastomers*, InTech, 2012.
- [91] S. S. Awanti, M. S. Amarnath, and a Veeraragavan, “Laboratory evaluation of SBS modified bituminous paving mix,” *J. Mater. Civ. Eng.*, vol. 20, no. 4, pp. 327–330, 2008.

- [92] S. S. Awanti, M. S. Amarnath, and A. Veeraragavan, "Influence of rest periods on fatigue characteristics of SBS polymer modified bituminous concrete mixtures," *Int. J. Pavement Eng.*, vol. 8, no. 3, pp. 177–186, 2007.
- [93] G. Wen, Y. Zhang, Y. Zhang, K. Sun, and Y. Fan, "Rheological characterization of storage-stable SBS-modified asphalts," *Polym. Test.*, vol. 21, no. 3, pp. 295–302, 2002.
- [94] N. . Lee, G. R. Morrison, and S. A. Hesp, "Low temperature fracture of polyethylene-modified asphalt binders and asphalt concrete mixes (with discussion)," *J. Assoc. Asph. Paving Technol.*, vol. 64, 1995.
- [95] P. Ahmedzade, M. Tigdemir, and S. F. Kalyoncuoglu, "Laboratory investigation of the properties of asphalt concrete mixtures modified with TOP-SBS," *Constr. Build. Mater.*, vol. 21, no. 3, pp. 626–633, 2007.
- [96] T. W. Kim, J. Baek, H. J. Lee, and J. Y. Choi, "Fatigue performance evaluation of SBS modified mastic asphalt mixtures," *Constr. Build. Mater.*, vol. 48, pp. 908–916, 2013.
- [97] B. Kim, R. Roque, and B. Birgisson, "Effect of Styrene Butadiene Styrene Modifier on Cracking Resistance of Asphalt Mixture," *Transp. Res. Rec.*, vol. 1829, no. 1, pp. 8–15, 2003.
- [98] T. W. Kim, J. Baek, H. J. Lee, and J. Y. Choi, "Fatigue performance evaluation of SBS modified mastic asphalt mixtures," *Constr. Build. Mater.*, vol. 48, pp. 908–916, 2013.
- [99] F. K. M. Hamed, "Evaluation of fatigue resistance for modified asphalt concrete mixtures based on dissipated energy concept," 2010.
- [100] H. Aglan, "Asphaltic Pavements . Part I : Effect of and Fatigue Behavior," *Polym. Addit. Their Role Asph. Pavements. Part I Eff. Addit. Type Fract. Fatigue Behav.*, vol. 25, pp. 307–321, 1993.
- [101] M. Aurilio, P. Mikhailenko, and H. Baaj, "Predicting HMA Fatigue Using the Double Edge Notched Tension Test and Multiple Stress Creep Recovery Test," in *Proceedings of the Sixth-Second Annual Conference of the Canadian Technical Asphalt Association (CTAA): Halifax, Nova Scotia, 2017.*
- [102] AASHTO, "Bulk specific gravity of compacted bituminous mixtures using saturated surface-dry specimens," AASHTO T-166, 2007.
- [103] W. Schütz, "A history of fatigue," *Eng. Fract. Mech.*, vol. 54, no. 2, pp. 263–300, 1996.
- [104] P. C. Hopman, P. Kunst, and A. C. Pronk, "A renewed interpretation method for fatigue measurements, verification of miner's rule," in *4th Eurobitume symposium in Madrid, 1989*, vol. 1, pp. 557–561.

- [105] A. C. Pronk, "Evaluation of the Dissipated Energy Concept for the Interpretation of Fatigue Measurements in the Crack Initiation Phase Report No P-DWW-95-001," Road Hydraul. Eng. Div. Rijkswaterstaat, Netherlands, 1995.
- [106] H. Soenen, C. de La Roche, and P. Redelius, "Fatigue behaviour of bituminous materials: from binders to mixes," *Road Mater. pavement Des.*, vol. 4, no. 1, pp. 7-27, 2003.

Appendices



Superpave Mix Design Report

AME - Materials Engineering, 10 Perdue Court, Units 2 - 3, Caledon, Ontario, Canada, L7C 3M6
 Phone: (905) 840-5914; Fax: (905) 840-7859, E-Mail: ame@amecorp.ca



LAB MIX NUMBER	13150.001 SP12.5FC2		JOB MIX FORMULA NO.	
CONTRACT NUMBER	Various	HOT MIX TYPE/USE	SP12.5FC2	ITEM NO.
HIGHWAY	Various Locations	LOCATION	Aecon - Hwy 407	
TESTING LAB	AME - Materials Engineering, Caledon, Ontario		DATE SAMPLES REC'D	06-Apr-15
TEST DATA CERTIFIED BY:			DATE COMPLETED	08-May-15

Job Mix Formula - Gradation Percent Passing *														
% AC	37.5	25	19.0	16.0	12.5	9.5	6.7	4.75	2.36	1.18	600	300	150	75
5.20	100	100.0	100.0	100.0	96.0	84.0		56.4	40.4	25.8	17.3	11.4	7.8	5.5

Traffic Category: D			Gyrations: N ini: 8 N des: 100 N max: 160		
Property	Requirements	Selected			
%Gmm @ N des / V%	96.5 / 3.5 ±0.3	96.2 / 3.8			
%Gmm @ N ini	89 Max	87.3			
%Gmm @ N max	98 Max	97.1			
% VMA	14 Min	16.1			
% VFA	65 - 78	76.2			
Dp	0.6 - 1.2	1.1			
TSR	80% Min	94.1			
% AGG #1	43.0	% RAP			
% AGG #2	13.0	% AC RAP			
% AGG #3	27.0	Consensus Properties			
%AGG #4	17.0	% CR Total	100.0		
% AGG #5		% CR 2 Face	100.0		
% AGG #6		% F & E (5:1)	1.8		
BRIQ. BRD	2.571	FAA	47.9		
MRD	2.673	Sand Equiv.	79		

ASPHALT CEMENT	
SUPPLIER	Grade
Yellowline	PG 58-28XV

ADDITIVE		
SUPPLIER	TYPE	AS % of AC
	N/A	

AGG. TYPE	SOURCE / INVENTORY NUMBER	AGG. TYPE	SOURCE / INVENTORY NUMBER
AGGREGATE #1	HL1 Stone / OTR Bruce Mines Quarry / B22-072	AGGREGATE #4	Screenings / OTR Bruce Mines Quarry / B22-072
AGGREGATE #2	Chip / Aecon Marmora Quarry / C01-058	AGGREGATE #5	
AGGREGATE #3	Washed DFC Fines / OTR Bruce Mines Quarry / B22-072	AGGREGATE #6	

AGGREGATE DATA	AGG. SPECIFIC GRAVITY	AGG. ABSORP. (%)	AGGREGATE GRADING - PERCENT PASSING												
			37.5	25	19.0	16.0	12.5	9.5	4.75	2.36	1.18	600	300	150	75
AGG #1	2.883	0.4	100.0	100.0	100.0	100.0	90.5	62.0	4.0	1.0	1.0	0.9	0.9	0.8	0.8
AGG #2	2.945	0.6						100.0	80.6	20.0	8.6	5.4	4.0	3.3	2.7
AGG #3	2.926	0.7						100.0	99.8	92.0	56.5	34.0	18.5	9.5	5.0
AGG #4	2.918	0.6						100.0	96.5	66.5	44.0	31.5	22.0	16.3	11.5
AGG #5															
AGG #6															
Coarse Agg. Gsb	2.892		Fine Agg. Gsb			2.915			Combined Gsb			2.905			

*JMF Adjusted to Allow for 2.0 % Fines Returned to the Mix

Remarks:

Mix Comp Temp=Recomp Temp=150 C; Wt Sample = 5125gms; Abs<2% no sealing required; AC Content by Ignition or Solvent; Mixing Temp=160C.

Reviewed By: _____

Date: _____



Moisture Sensitivity Data

AASHTO T 283

Additive: None AC %: 5.2 Design: 13150.001 SP12.5FC2
 PGAC: 58-28XV
 Date Completed: 07-May-15 Project: Hwy 407

Sample	1	2	3	4	5	6
Diameter, mm	150	150	150	150	150	150
Thickness, mm	95.7	95.7	95.7	95.7	95.7	95.7
Dry Mass, gm	4077.7	4072.1	4078.8	4082.3	4077.2	4080.6
SSD Mass, g	4101.5	4106	4109.5	4112.7	4102	4109.2
Mass in Water	2457.5	2462.4	2466	2463.8	2454.3	2470.1
Volume, cc	1644	1643.6	1643.5	1648.9	1647.7	1639.1
Bulk Sp Gravity	2.480	2.478	2.482	2.476	2.474	2.490
Max Sp Gravity	2.673	2.673	2.673	2.673	2.673	2.673
% Air Voids	7.2	7.3	7.2	7.4	7.4	6.9
Vol Air Voids	118.5	120.2	117.6	121.7	122.4	112.5
Load, N				12500	11250	11000
Saturated						
SSD Mass, gm	4169.3	4166	4169.6			
Vol Abs Water, cc	91.6	93.9	90.8			
% Saturation	77.3	78.1	77.2			
Conditioned						
Load, N	10800	11500	10400			
Dry Str				555	499	488
Wet Str	479	510	461			
Average Dry Strength (kF)	514					
Average Wet Strength (k)	484					
%TSR	94.1%					

